Applications of Real-Time GNSS-RF and Lidar-Derived Products to Improve Forest Operations in Beetle-Killed Stands in the Inland Northwest

A Thesis

Presented in Partial Fulfilment of the Requirements for the

Degree of Master of Science

with a

Major in Natural Resources

in the

College of Graduate Studies

University of Idaho

by

Ryer M. Becker

Major Professor: Robert F. Keefe, Ph.D.

Committee Members: Nathaniel Anderson, Ph.D.; Jan U.H. Eitel, Ph.D.

Department Administrator: P. Charles Goebel, Ph.D.

December 2017

Authorization to Submit Thesis

This thesis of Ryer M. Becker, submitted for the degree of Master of Science with a major in Natural Resources and titled "Applications of Real-Time GNSS-RF and Lidar-Derived Products to Improve Forest Operations in Beetle-Killed Stands in the Inland Northwest," has been reviewed in final form. Permission, as indicated by the signatures and dates below, is now granted to submit final copies to the College of Graduate Studies for approval.

Major Professor: ______________________ Date: __________
Robert F. Keefe, Ph.D.

Committee Members: ______________________ Date: __________
Nathaniel Anderson, Ph.D.

______________________ Date: __________
Jan Eitel, Ph.D.

Department Administrator: ______________________ Date: __________
P. Charles Goebel, Ph.D.

Abstract

Forest management has encountered fast-paced evolution integrating technologies and data sources which have in turn helped mold a new paradigm of forestry focused on site specific management strategies rather than one size fits all management. Using real-time, consumer-grade GNSS-RF transponders was found to successfully classify productive cycle elements of a forestry machine over 90% of the time, showing the effectiveness of spatially explicit data in defining cycle elements for production analysis. Additionally, lidar-derived forest metric predictions, exceeding 70% accuracy, were used to develop a harvest system classification model. Alternative harvest systems (shovel harvester; tethered shovel) were determined to be feasible alternatives to traditional harvest systems across a statistically significant proportion of study site stands and hectares when investigating varying harvest system combinations. These initial studies set groundwork for refining and expanding our analyses as we continue to explore integration of real-time data and high resolution spatial data in forest operations.

Acknowledgements

I would like to thank my major professor, Dr. Robert F. Keefe, for his continued support and encouragement throughout the completion of this thesis. His mentorship, leadership and passion for research pushed me to expand my professionalism, strive for excellence and foster a desire to continue to conduct research into the future as I continue in my career. This project would not have reached the level of success it has without his support and contributions. I would also like to thank my committee members for all they have done. I would like to thank Dr. Nathaniel Anderson for his guidance and input from the very early stages of the project through the completion with his expertise in forest operations. Additionally, I would like to thank Dr. Jan Eitel for his expertise and support in the remote sensing analysis portion of my work.

I would like to thank the Nez-Perce Clearwater National Forest and the USDA Forest Service Laboratory in Moscow, ID for all their support and help in providing necessary spatial data and facilitating us during field sampling. There are many individuals whose help was invaluable throughout the various stages of the project. Additionally, I would like to extend the deepest thanks to the USDA AFRI and members of the BANR project for funding this research. This project was funded by the Agriculture and Food Research Initiative Competitive Grant no. 2013-68005-21298 from the USDA National Institute of Food and Agriculture. I would also like to thank all the loggers and contractors we worked with for helping facilitate our field work and experiments. This work would not have been possible without your help.

Dedication

I would like to dedicate this work to my family and friends for all their support and endless encouragement through the entirety of this process. Specifically, thanks to my parents and grandparents for being my biggest supporters along the way and always pushing me to pursue my dreams and grow as a forester, researcher and overall human being. I would not be here today without all you have taught me and the values you have instilled in me throughout my life. For all those not mentioned, know your support and encouragement throughout this process has been greatly appreciated.

Table of Contents

List of Tables

List of Figures

Chapter 1: Introduction: Improving precision forestry with new developments in location technology and remote sensing

1.1 Introduction

Logging production and costs are central to determining the feasibility of timber harvesting operations. With changing management regimes and innovative harvest machinery and techniques being introduced, the means to assess and plan for these variables must be developed. Advances in spatially explicit, real-time data and remotely sensed imagery provide valuable opportunities to augment existing decision-making tools for forest operations to aid land managers and harvest planners. These advancing technologies and data resources are part of a larger narrative and expanding field of precision forestry. Understanding the ways in which to incorporate these tools into management strategies will help improve the overall effectiveness, safety, and sustainability of land management practices and actualize the conceptual goals of precision forestry.

1.2 GNSS-RF Technology and Opportunities

Real-time GNSS-RF (global navigation satellite system with radio frequency) technology is a promising area of development and research for use in forest management, logging safety and wildland fire applications (Keefe et al. 2014). GNSS uses satellites from various systems (GLONASS, GPS, Galileo) to provide positional data to receiving units. However, these data are generally stored within the unit and must be downloaded at a later date. By incorporating radio frequency transponders into the GNSS units, data can be shared between units in real-time, allowing for data sharing capabilities previously unavailable with GNSS. Radio frequency transmission and data sharing remains possible outside of internet or cellular networks, making this technology a valuable resource in remote areas where logging operations regularly occur.

Manually recorded elemental cycle time studies have served as the basis for many time and production studies, using observed data to determine production and subsequent costs. However, GNSS-RF technology provides a promising alternative to traditional time study methods. For both research and operational applications, developing relationships between machine movements, GNSS-RF data and determining the accuracy at which machine elements can be classified from spatially explicit data is crucial. These activity profiles define work of various harvest and forest management tasks at individual cycle elements.

An initial step in the process of developing these activity profiles entailed determining the accuracy at which GNSS-RF transponders were able to record and classify the swing movements of a log loader. In Chapter 2 of this thesis, these primary assessments were performed to create a base of knowledge for future development of an activity profile that quantifies shovel movements based on two or more GNSS positions transmitted at high frequency. The activity profile developed for the swing of the log loader was a necessary initial step in developing a larger library of machine elements derived from GNSS-RF data.

This study was performed using three varying transmission rates of data packets (2.5, 5.0 and 10.0 seconds) for GNSS-RF transponders at two locations along the machine boom and two cycle elements when swinging to 18 pre-determined angle segments. The 2.5 second transmission rate was found to be the most successful in correctly classifying the productive cycle elements, followed closely by the 5.0 second transmission rate which was significantly similar. The transponders located at the end of the boom also returned higher proportions of correctly classified elements than the transponder located on the heel rack for the 2.5 and 5.0

second transmission rates. Observed swing angles were also most accurately captured by the 2.5 second return interval as expected. Consumer-grade GNSS-RF transponders were shown to accurately and effectively capture the movements of a log loader and provide the data necessary to classify productive cycle elements.

1.3 New Applications of Remotely Sensed Products in Forest Operations

In addition to advancements in real-time GNSS-RF technologies and their application in forest operations, remotely sensed data is another avenue of innovation for precision forestry. Terrestrial or mobile laser scanning and airborne and space-borne point clouds provide various means to collect high resolution spatial data with varying degrees of data density and accuracy; each with their own respective scope of use (Holopainen et al. 2014). Airborne laser scanning (ALS), also known as lidar, allows for the derivation of three-dimensional vertical forest structure characterization and is capable of producing high accuracy forest attribute predictions and highly resolution digital elevation models (Jusoff 2009; White et al. 2013).

High-resolution lidar has been used widely in forest inventory and biometrics research. Lidar products provide valuable insight into forest growth, canopy characteristics and vegetation dynamics (Reutebuch et al. 2005; Smith et al. 2014). However, use of lidar data in the context of forest operations has been limited. Road layouts using high resolution digital elevation models derived from lidar has been a commonly used application of these data (Akay et al. 2004; Aruga et al. 2005; Akay and Sessions 2005; Akay et al. 2009). Lidar has been used to assess the impacts of forest harvest landings on future regrowth, provide pre-harvest assessment into potential harvest blocks and identify areas disrupted by selective harvesting operations (Heinimann and Breschan 2012; d'Oliveira et al. 2012; Slesak and Kaebisch 2016; Ellis et al. 2016). Additionally, lidar has also been used to predict harvest production by developing relationships between lidar-derived forest characteristics and time and motion production data (Alam et al. 2011).

In Chapter 3, we utilized lidar-derived forest and topographic characteristics to develop a decision support system for harvest system selection at the landscape scale. Spatial data were used to define feasible harvest systems at the stand level for varying harvest scenarios and combinations of equipment. Three harvest scenarios representing three varying combinations of harvest systems were assessed to determine the impact of introducing innovative, alternative harvest systems at the landscape scale. Operational thresholds were defined for each of the harvest systems, representing areas where the system could feasibility operate within the context of forwarding distance, ground slope, and merchantable volume. The two alternative harvest systems analyzed (shovel harvester and tethered shovel) were found to represent significant proportion of stands and hectares previously classified as feller-buncher and excaliner ground respectively. These results will aid forest harvest managers in the decision-making process pertaining to the selection of harvest systems based on operational thresholds of individual harvest systems and the correlating forest and topographic characteristics of a harvest area.

These foundational studies addressed in the following two chapters establish the basis for future studies that further expand on current methods and results. Activity profiles derived from the GNSS-RF data and the associated methods are subsequently being developed into algorithms that model shovel and other equipment movements during operational harvesting. This will aid future research as we continue to explore traditional and innovative technological support of harvest optimization. Additionally, these activity profiles will be incorporated into the decision support model for harvest system selection to further strengthen its capabilities.

While the model currently determines all the feasible harvest systems for a group of stands at the landscape scale, incorporating activity profiles into the model will introduce simulation and production analysis capabilities. With this, optimal harvest system selection analysis will be performed at the landscape scale using lidar-derived forest and topographic metrics and GNSS-RF derived activity profiles.

The use of real-time positioning systems in forestry, integrating Global Navigation Satellite System (GNSS) and radio frequency (RF) devices, is growing and is important for the advancement and development of operational precision forestry (Keefe et al. 2014; Grayson et al. 2016). The ability to define relevant forest management and products information and link them to geographic locations using advanced data and technology is advantageous to sustainable forest management. Precision forestry is an intensive management technique that emphasizes development of operational practices that incorporate technologies and processes to increase productivity, reduce costs, and reduce negative site impacts, especially those on vegetation, soil, and water resources (Veal et al. 2002; Kovacsova and Antalova 2010). This management process focuses on incorporating site specific spatial and attribute data through the application of technology for environmentally and operationally sound forest management operations (Eker and Ozer 2015). Veal et al. proposed separating precision forestry into two main categories: using GIS and spatial data to aid forest management and planning and; site specific silvicultural prescriptions and applications (2002). Precision forestry concepts provide highly repeatable measurements, actions and processes and enables sharing of information between resource managers and other stakeholders gathered from advanced technologies and data (Kovacsova and Antalova 2010).

Advancements in GIS, GNSS, light detection and ranging (lidar), real-time analysis, and most recently GNSS-RF has led to increased interest and application of precision forestry techniques (Kellndorfer et al. 2003; Aruga 2003; Zhang et al 2014). The innovative application of these new technologies and data sources opens the door for advancements in operational forestry by increasing efficiencies of forest management activities and providing real-time feedback to operators and managers (Carter et al. 1999; Hamzah 2001). As precision forestry and associated areas of study continue to advance and expand, steps to incorporate new technologies and innovative uses of remotely-sensed data will become more prevalent in operational settings. Forest managers and harvest planners will continue to have tools and resources made available to aid in the decision-making process. The ability to define the applications for which new data and technologies will be applied in the context of precision forestry is important in addressing the challenges faced in forestry and fully recognizing the potential of precision forestry as a management strategy (Farnum 2001).

The following two chapters introduce innovative applications of high resolution remotely sensed data and real-time positional data for forest operations. These studies extend further than simply describing the value and utility of these data sources, but provide insight into their application in decision support products to address management challenges and the way in which precision forestry is incorporated into real world management scenarios. In turn, this may change the way in which management decisions are made, work is defined and increase the production of logging operations in the Western United States and beyond. Maximizing logging production through improved decision making and optimal harvest system selection, while valuable in all forest operations, is especially so in salvage harvests from fire and insect infestations where value degradation and low value products decrease harvest feasibility for these sites. In the Inland Northwest, mountain pine beetle has caused extensive mortality leading to challenges regarding harvest scheduling and selecting management strategies to address the millions of affected acres. Technology and high resolution spatial data integration through decision support tools provide a means to aid developing management strategies which encourage the current and future sustainability of our forest resources.

1.4 References

Akay AE, Karas IR, Sessions J, Gundogan R. 2004. Using high-resolution digital elevation model for computer-aided forest road design. Proceedings of the International Society of Photogrammetry and Remote Sensing Congress; July; Istanbul, Turkey.

Akay AE, Oguz H, Karas IR, Aruga K. 2009. Using LiDAR technology in forestry activities. Environ Monit Assess. 151:117-125.

Akay AE, Sessions J. 2005. Applying the decision support system, TRACER, to forest road design. W J App For. 20(3):184-191.

Alam M, Strandgard M, Brown M, Fox JC. 2011. Harvesting productivity analysis using lidar. Proceedings of the 11th International Conference on LiDAR Applications for Assessing Forest Ecosystems; October 16-20; Tasmania, Australia.

Aruga K. 2003. Precision forestry operations and equipment in Japan. Proceedings of the Second International Precision Forestry Symposium; June 15-17; Seattle, WA.

Aruga K, Sessions J, Akay AE. 2005. Application of an airborne laser scanner to forest road design with accurate earthwork volumes. J For Res. 10:113-123.

Carter EA, McDonald TP, Torbert JL. 1999. Application of GPS technology to monitor traffic intensity and soil impacts in a forest harvest operation. Proceedings of the Tenth Biennial Southern Silvicultural Research Conference; February 16-18; Shreveport, LA.

d'Oliveira MVN, Reutebuch SE, McGaughey RJ, Andersen H. 2012. Estimating forest biomass and identifying low-intensity logging areas using airborne scanning lidar in Antimary State Forest, Acre State, Western Brazilian Amazon. Remote Sens of Env. 124:479-491.

Eker M, Ozer D. 2015. Precision forestry in forest harvesting: Conceptual framework. Turkish J For. 16(2): 183-194.

Ellis P, Griscom B, Walker W, Goncalves F, Cormier T. 2016. Mapping selective logging impacts in Borneo with GPS and airborne lidar. For Ecology and Management. 365:184-196.

Farnum P. 2001. Precision forestry- finding the context. In Proceedings of the First International Precision Forestry Symposium; June 20-21; Seattle, WA.

Grayson LM, Keefe RF, Tinkman WT, Eitel JUH, Saralecos JD, Smith AMS, Zimbelman EG. 2016. Accuracy of WAAS-Enabled GPS-RF warning signals when crossing a terrestrial geofence. Sensors. 16:1–8.

Hamzah KA. 2001. Remote sensing, GIS and GPS as a tool to support precision forestry practices in Malaysia. Proceedings of the 22nd Asian Conference on Remote Sensing; November 5-9; Singapore.

Heinimann HR, Breschan J. 2012. Pre-harvest assessment based on lidar data. Croat J For Eng. 33(2):169-180.

Holopainen M, Vastaranta M, Hyyppa J. 2014. Outlook for the next generation's precision forestry in Finland. Forests. 5(7):1682-1694.

Jusoff K. 2009. Precision forestry using airborne hyperspectral imaging sensor. J Ag Science. 1(1):142-147.

Keefe RF, Eitel JUH, Smith AMS, Tinkham WT. 2014. Applications of multi-transmitter GPS-VhF in forest operations. Proceedings of the 47th International Symposium on Forestry Mechanization and 5th International Forest Engineering Conference; September 23-26; Gerardmer, France.

Kellndorfer JM, Dobson MC, Vona JD, Clutter M. 2003. Toward precision forestry: Plot-level parameter retrieval for slash pine plantations with JPL AIRSAR. IEEE Transactions on Geoscience and Remote Sensing. 41(7):1571-1582.

Kovacsova P, Antalova M. 2010. Precision forestry- definition and technologies. Sumarski List. 134(11):603-611.

Reutebuch SE, Andersen H, McGaughey RJ. 2005. Light detection and ranging (lidar): An emerging tool for multiple resource inventory. J For. 103(6)286:292.

Slesak RA, Kaebisch T. 2016. Using lidar to assess impacts of forest harvest landings on vegetation height by harvest season and the potential for recovery over time. Can J For Res. 46:869-875.

Smith AMS, Falkowski MK, Greenberg JA, Tinkham WT. 2014. Editorial: Remote sensing of vegetation structure, function and condition: Special issue. Remote Sens of Env. 154:319-321.

Taylor SE, Veal MW, Grift TE, McDonal TP, Corley FW. 2002. Precision forestry: Operational tactics for today and tomorrow. Proceedings of the Council on Forest Engineering (COFE); Auburn, AL.

White JC, Wulder MA, Vastaranta M, Coops NC, Pitt D, Woods M. 2013. The utility of image-based point clouds for forest inventory: A comparison with airborne laser scanning. Forests. 4(3):518-536.

Zhang H, Zheng J, Dorr G, Zhou H, Ge Y. 2014. Testing of GPS accuracy for precision forestry applications. Arab J Sci Eng. 39:237-245.

Chapter 2: Use of real-time GNSS-RF data to characterize the swing movements of forestry equipment

Published In:

Becker RM, Keefe RF, Anderson NM. 2017. Use of real-time GNSS-RF data to characterize the swing movements of forestry equipment. Forests. 8(2):44.

2.1 Abstract

The western United States faces significant forest management challenges after severe bark beetle infestations have led to substantial mortality. Minimizing costs is vital for increasing the feasibility of management operations in affected forests. Multi-transmitter Global Navigation Satellite System (GNSS)-radio frequencies (RF) technology has applications in the quantification and analysis of harvest system production efficiency and provision of real-time operational machine position, navigation, and timing. The aim of this study was to determine the accuracy with which multi-transmitter GNSS-RF captures the swinging and forwarding motions of ground based harvesting machines at varying transmission intervals. Assessing the accuracy of GNSS in capturing intricate machine movements is a first step toward development of a real-time production model to assist timber harvesting of beetle-killed lodgepole pine stands. In a complete randomized block experiment with four replicates, a log loader rotated to 18 predetermined angles with GNSS-RF transponders collecting and sending data at two points along the machine boom (grapple and heel rack) and at three transmission intervals (2.5, 5.0, and 10.0 s). The 2.5 and 5.0 s intervals correctly identified 94% and 92% of cycles at the grapple and 92% and 89% of cycles at the heel, respectively. The 2.5 s interval successfully classified over 90% of individual cycle elements, while the 5.0 s interval returned statistically

similar results. Predicted swing angles obtained the highest level of similarity to observed angles at the 2.5 s interval. Our results show that GNSS-RF is useful for real-time, model-based analysis of forest operations, including woody biomass production logistics.

2.2 Introduction

Real-time data analysis using Global Navigation Satellite System (GNSS) positioning coupled with data communication over radio frequencies (RF), or GNSS-RF, is an area of increasing interest in harvest operations as this new technology creates opportunities for innovation in operational forestry. Real-time data analysis and decision support may also be useful in the context of woody biomass logistics as new markets for forest residues and salvage wood develop. Increased interest in emerging and existing bioenergy markets is closely linked with reducing the risks that forested lands face from fire, insects, and pathogens (Wells et al. 2015). It has been estimated that 15 western states in the US contain over 11 million hectares of forested land that could benefit from treatments to improve resilience and health by initiating active forest management on the landscape (Rummer and Prestemon 2003). In order to return stands to historic stand dynamics and improve forest health, silvicultural treatments need to be performed, even in stands where such treatments generate large amounts of residues and primarily yield low value products (Brown et al. 2004).

Despite increased interest and developing markets, and because biomass products from forest residues are generally low in value, landowners and contractors must develop efficient, effective, and sustainable methods for harvesting and gathering forest residues and beetle-killed timber or the long-term feasibility of supporting new wood-based bioenergy markets will be limited (Anderson et al. 2012). By 2022, it is estimated that 12.4 million dry tons of forest residues will be available annually to be utilized for bio-energy (Jacobson et al. 2016).

Higher production rates and lower costs associated with logging systems used in silvicultural systems for salvage and forest restoration operations, including the gathering and processing of other forest residues, will allow forest managers to treat more forest land at lower costs and access a higher proportion of this available biomass feedstock. Not only could this result in healthier forests, but the increased feedstock supply for bioenergy and bio-based product manufacturing could help bolster the economies in communities that rely heavily on the forest products industry. Historically in the US, forest residues have been the primary fuel for bioenergy production, with industrial process heat and power production from forest biomass representing a large portion of overall renewable energy production. Epidemic outbreaks of the mountain pine beetle (*Dendroctonus ponderosae* Hopkins) and subsequent mortality of millions of hectares of lodgepole pine (*Pinus contorta* var. *latifolia* Engelm.) in the northern Rocky Mountains has led to an increased interest in utilizing associated biomass as a bioenergy feedstock option (Anderson and Mitchell, 2016). Identifying harvesting and processing methods that increase production efficiency and reduce costs through real-time positional analysis of operational equipment and workers may increase the feasibility of using forest residues from treatments in beetle-killed timber, as well as improve overall operational efficiency. Harvesting these degraded beetle-killed stands helps promote the reintroduction of healthy, sustainable forests. The ability to accurately define specific machine elements from spatial data acquired from GNSS-RF transponders is a necessary and first step for the development of real-time production analysis and operator decision-support models that would help achieve these goals.

In the western US, a major potential supply of biomass is thinning residues and other materials removed from fuel treatment operations that occur on US national forests (Keefe et al. 2014b). Incorporating GNSS-RF technologies in innovative ways in the forest industry may assist operations foresters and contractors in determining the best processes and methods for timber harvesting through real-time positioning and production logistic modeling, especially in beetle-kill. For example, real-time analysis can help to optimize on-the-fly skid trail layout, the order of harvesting, skidding, and processing, and placement of intermediate feedstock preprocessing depot locations.

The on-board data loggers that are standard equipment in many modern forest machines record several types of data that may be useful for real-time analysis of production, such as log piece size and numbers of stems processed (Palander et al. 2013; Strandgard et al. 2013). The addition of discrete equipment position, navigation, and timing (PNT) information to the standard data stream would make it possible for operators to account for and adapt to unforeseen delays in machine cycles or site conditions. Experienced operators do this naturally over short time steps on the fly, but computer-aided analysis can help expose patterns in operation that are not always apparent, even to the most experienced personnel. Utilization of real-time position data for individual pieces of equipment and among multiple pieces of equipment in a system could make it possible for higher resolution and higher order complexity operational models that monitor individual equipment cycle elements and suggest efficiency improvements based on variables like terrain, timber quality, and other site characteristics (Palander et al. 2013; Strandgard et al. 2013).

GNSS technology has been studied and in some cases employed in operational forestry contexts including thinning stands, tracking movements of site preparation machinery, aligning logging roads, and positioning and dispatching log trucks along haulage routes in real-time, as well as characterizing soil disturbances related to harvest operations (Devlin and McDonnell

2009; Carter et al. 1999; Danskin et al. 2009; Hamzah 2001). Recently, the use of real-time positioning systems in forestry that employ integrated Global Navigation Satellite System (GNSS) and radio frequency (RF) devices is growing, and is important for the advancement and development of operational precision forestry (Keefe et al. 2014a; Grayson et al. 2016). Precision forestry is an intensive management technique that emphasizes development of operational practices that incorporate technologies and processes to increase productivity, reduce costs, and reduce negative site impacts, especially those on vegetation, soil, and water resources. Advancements in GIS, GNSS, light detection and ranging (LiDAR), real-time analysis, and most recently GNSS-RF has led to increased interest and application of precision forestry techniques. The innovative application of these new technologies opens the door for advancements in operational forestry by increasing efficiencies of forest management activities (Carter et al. 1999; Hamzah 2001). GNSS uses satellites from the U.S. Global Positioning System (GPS), the Russian global navigation satellite system (GLONASS), and possibly other satellite systems to offer spatial reference data to GNSS receivers around the world. Positioning relies on GNSS receiver ability to communicate with satellite systems to provide location data and is used widely across the globe in consumer, military, and industrial applications. RF are electromagnetic wave frequencies in the range commonly used for communication and radar signals. When GNSS is paired with RF (GNSS-RF) the resultant system has the capability to utilize multiple GNSS-RF transponders that receive positional data through GNSS signals and then instantaneously relay information through RF devices to a receiver. Additionally, communication between transponders and receivers is not reliant on cellular networks nor internet connectivity (Keefe et al. 2014a). This is especially important for real-time positioning applications in forest operations, which often occur in remote areas with limited cellular network coverage.

Earlier work has primarily focused on GNSS positioning technologies that relay the location of equipment to a distant computer, as with dispatch systems deployed in transportation (Devlin and McDonnell 2009) and service monitoring applications included on modern machinery. Real-time systems that communicate equipment and ground-worker locations among one another locally at remote logging sites are an important advancement because the technology opens the door to integrated, simultaneous analysis of data from multiple machines and ground workers interacting with one another within the framework of computer-augmented decision processes, with the objective of improving production logistics and safety (Keefe et al. 2014a; Grayson et al. 2016).

Past research has returned promising results related to the ability of GNSS receivers to monitor forestry equipment movements, though dense forest canopies are known to increase GNSS error and reduce the ability to collect precise and accurate measurements in dense stands (Devlin and McDonnell 2009; Sigrist et al. 1999; Hasegawa and Yoshimura 2007; Taylor et al. 2001; Veal et al. 2001; Yoshimura and Hasegawa 2003). Even when accuracy is reduced due to canopy closure, GNSS can be successful when high accuracy in monitoring object movements is not required (Devlin and McDonnell 2009). For example, position accuracy to 10 meters may be insufficient for safety applications, but acceptable for transportation routing. Landscape topography has also been an obstacle in the use of GNSS in forestry applications due to line of sight obstructions (Wing et al. 2005). McDonald and Fulton (2005) used GNSS for elemental analysis of skidder cycles and found that GNSS locations could successfully be used to predict cycle durations and distinguish between different elements within those cycles (e.g., grapple, positioning, and travel), though the system was subject to large errors when compared to clock studies (i.e., manual timing by an observer) with regard to specific element durations. Operational cycles measured with GNSS agreed with direct observation times 90% of the overall time studied (McDonald and Fulton 2005). Similar accuracies were found when using GNSS transponders to analyze the cycle times of forwarders and when using vibration sensors to assist in the determination of cycle times (Strandgard and Mitchell 2015).

While GNSS data have been effective for capturing the location, movements, and overall cycle times of some forest machinery, researchers have encountered problems when attempting to acquire high levels of accuracy in the analysis of specific productive cycle elements (McDonald and Fulton 2005; Strandgard and Mitchell 2015; Wang et al. 2003; De Hoop and Duprè 2006). Additionally, there has been limited prior research evaluating the quality of productive cycle element characterization using positional information derived from GNSS-RF data. Understanding the accuracies and capabilities of commercially available, consumer-grade GNSS-RF transponders will facilitate development of their application in beetle-killed harvest logistics and in production analysis in forest operations more broadly.

The objective of this study was to determine the effectiveness of multi-transmitter GNSS-RF units for characterizing the cycle elements of a log loader at three intervals of GNSS-RF signal transmission and two locations along the machine boom, using time and positional data sent by the transponders. GNSS-RF positional data were compared statistically to manually recorded time intervals for the same cycle elements. Our goals in determining the accuracy of the technology were two-fold: (1) to foster innovation in operations research, especially in the safe, efficient characterization of cycle elements and continued development of accurate, real-time model-assisted decision support and analysis; and (2) to facilitate the development and deployment of these technologies in the forest sector to improve productive efficiency and reduce costs. These goals are of particular interest and application in improving harvest logistics of beetle-killed timber harvests for biomass when product values are low, potential profit margins are narrow, and cost-minimization, even by small margins, can have large impacts on the financial viability of supply chains.

2.3 Materials and Methods

We used Garmin Alpha multi-transmitter GNSS-RF units to record the swing movements of a stationary log loader, also called a “shovel”, in order to characterize the swinging and slew of the boom. This study was conducted on one research site with four replicated trials, with each trial consisting of 18 cycles. The full swing extent of the machine (360 degrees) was broken into 18 equal arc segments of 20 degrees each (Figure 1). Separation of the swing extent into smaller components made it possible to time the machine movements at varying swing angles to determine if GNSS-RF transponders were able to capture the machine movements accurately at different distances of motion. This was done for three transmission frequency refresh intervals: 2.5, 5.0, and 10.0 s. These three refresh intervals translate into transmission intervals of 24, 12, and 6 transmissions per minute for the 2.5, 5.0, and 10.0 intervals respectively. GNSS-RF transponders were placed in three locations on the machine: one in the right-rear of the cab (close to the center of the machine), one at the full boom extent near the grapple, and one at the heel rack, which is halfway down the most forward boom segment (Figure 2.1).

To lay out the experiment, a circle with a radius of 12.2 m was delineated in a flat, open area. The open area was chosen purposefully to avoid attenuated GNSS signals and resulting multipath error. The center point was chosen and a fiberglass tape was extended to the chosen radius or 12.2 m. As the individual at the center point rotated around the axis, a field technician on the end of the tape marked the outside edge with paint. Wooden stakes were placed along the circumference of the circle to mark the 18 different angle segments of 20 degrees each. To determine the location of these points, we determined the side length of an octdecagon (18-sided regular polygon) using the circumradius of 12.2 meters and the formula side = 2 r sin (180/*n*), where "*r*" is the circumradius, and "n" is the number of sides. Each side of the polygon measured 4.23 m. A starting point stake labeled "0" was placed on the circumference of the circle. The location of stake 1 was determined by measuring 4.2 m from stake 18 and finding where along this circumference of the circle this landed. This process was repeated for the remaining stakes (2–17) until there were 18 unique 20-degree angle segments within the full swing extent as shown in Figure 2.1.

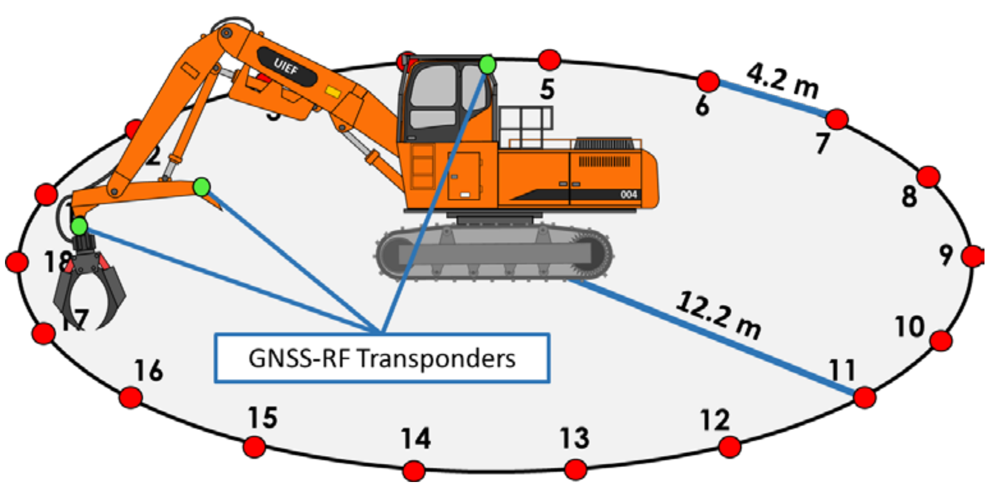

Figure 2.1 Study layout, consisting of eighteen, twenty-degree shovel swing angle segments.

The machine was then driven to the center of the plot and operated in this location for the duration of the study. Keeping the machine in a stationary position removed any possible error or variation that lateral movements would introduce to the GNSS data. The signal sent to the hand-held receiver relies on satellite communication to transmit GNSS locations. The number of satellites with which the receiver can communicate at any point in time alters the accuracy of the measurement at that time, meaning accuracy is variable in time depending on how many satellites are in range. We were not able to record the number of satellites in range for each measurement to quantify this source of error. Therefore, a completely randomized design was used in the data collection process, which is described below. A total of seven (7) Alpha multi-transmitter GNSS units were used for the experiment and two (2) handheld receivers were used in data collection. Three Alpha transponders were utilized in measuring the boom movements at the grapple head and were labeled Boom 1, Boom 2, and Boom 3. Boom 1, 2, and 3 were assigned transmission intervals 2.5, 5.0, and 10.0 s, respectively. Three additional Alpha transponders were used in the data collection for the heel rack and labeled Heel 1, Heel 2, and Heel 3 with transmission intervals 2.5, 5.0, and 10.0 s, respectively. One Alpha transponder was labeled as Cab and was used for both the boom and heel trials. The main hypothesis being tested is that shorter transmission intervals result in better accuracy when classifying cycle elements. Additionally, we hypothesized that shorter intervals would also result in more accurate estimates of the angle of machine swing.

The three Alpha transponders attached to grapple and the cab transponder were synched to one handheld receiver. The additional three transponders for the heel and the cab transponder were synched to the second handheld receiver. Two handheld receivers (full and heel) were used as opposed to one receiver to ensure data would not overlap and be compromised. During the swinging experiment, the boom was extended to 9.5 m from the center axis of the log loader and the heel rack was kept a constant 6.7 m from the center axis of the log loader. After each replicated trial, these distances were checked to ensure consistency throughout the experiment.

The transponders were easily attached to the heel rack and grapple of the loader with zip-ties, meaning no modifications had to be done to the machinery and the operator could perform tasks normally, with no changes in operation attributable to the addition of the transponders or any other experimental condition.

In each of the four trials, the shovel covered all 18 of the angle segments in separate cycles in random order predetermined by a random number generator. Through each of the 18 cycles per trial, the start time, stop time at the randomly selected angle, and the return time to the start position was recorded both manually and through the data packets received by the GNSS-RF receiver. Manual timing was conducted on a laptop computer using the Sys.time() command in the R statistical programming environment. The internal clock of the laptop used to conduct the manual timing was synched to the time on the GNSS-RF receiver by synchronizing with the nist.gov time server (NIST Internet Time Servers 2016). Synching the time of the GNSS-RF receivers and the laptop assisted in matching the GNSS-RF data with the manually recorded cycle times ensuring error when merging manually and remotely collected data was minimized.

Three 4.9 m, beetle-killed lodgepole pine logs were used in the experiment to simulate real world use of the loader on a harvest site. For each of the 18 cycles for each of the four replications, the same sequence was followed. This resulted in 72 unique cycles for both the grapple and heel rack GNSS placements. The logs and log loader boom began at the 0 degree marker to start each cycle. Once the operator swung to the required angle, the logs were dropped and the loaded swing time was recorded. The operator would then swing back to the starting position empty, following the same path. The ending time was recorded when the grapple was placed on the ground back at position 0. At this time the operator would then gather the logs and return them to the 0 degree marker to reset for the next cycle, which always started at position 0. Two cycle elements were defined to represent the movements of the log loader: “Swing/Unload” and “Return”. “Swing/Unload” is described as the time from the start of the swing for each cycle with a loaded grapple starting at angle 0 until the loader drops the logs at the ending angle measure and starts the swing back to the starting point. At this point, the time from the start of the return swing to the moment the grapple touches the ground back at angle 0 is defined as “Return”. The loading element of the cycle, which consists of an unloaded grapple leaving the stop position and collecting logs before the start of the loaded swing element was not included in measurement because it was expected to be identical for each cycle, was not required to test transponder accuracy, and would have introduced additional variation into the timing. Motorola two-way radios were used to communicate with the operator during the experiment, including directions about the selected angle for each cycle.

The resulting data from the field observation data sheets and the data received from the Garmin GNSS-RF receivers were entered into a spreadsheet and imported into the statistical analysis environment “R”. The data were then processed, analyzed, and interpreted following the flow diagram represented in Figure 2.2.

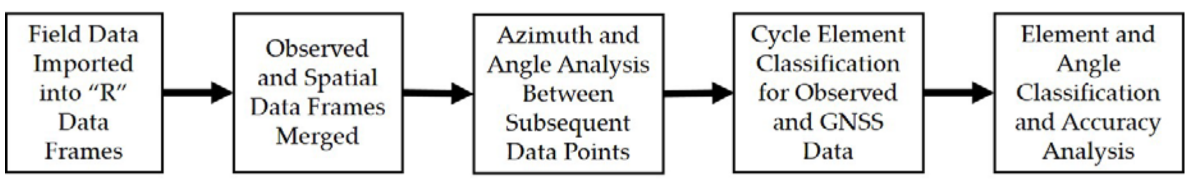

Figure 2.2 Flow diagram showing the progression of analysis of the spatial and observed data.

A chi-squared ANOVA test was performed to determine the significance of each individual parameter on the proportion of correct classifications. The parameters tested included transmission interval, swing angle, transponder location, cycle element, and the interaction of transmission interval and swing angle. Additionally, a binomial logistic regression was used to determine the influence of the predictor variables on cycle element classification of the

GNSS data when compared to the field observations. A regression based two-one sided *t*-test (TOST) equivalence test was performed to analyze whether the predicted angles of the model derived from GNSS-RF data were statistically similar to the observed angle measures. To further analyze the relationship between observed and predicted angle measures derived from the GNSS-RF data, a linear regression based adapted two-one sided *t*-test (TOST) was performed with bootstrapping in order to determine whether the null hypothesis of dissimilarity could be rejected for the observed angle measures and predicted values. Unlike traditional hypothesis testing where a failure to reject null results in a conclusion of indifference, an equivalence test starts with the assumption of dissimilarity, meaning that a rejection of null indicates similarity. This analysis process then shifts the burden of proof onto the model's ability to derive accurate predictions. Equivalence testing was originally derived from bioequivalence testing used in the development of pharmaceutical drugs, and has been successfully adapted and utilized in tree physiology and biometrics research (Robinson and Froese 2004; Robinson et al. 2005). While TOST tests for population-wide agreement, the regression based adaptation discussed by Robinson et al. also addressed point to point agreement between observed and predicted values (Robinson et al. 2005). This adapted analysis is able to test how well the distributions of the observed angles match the distribution of the predicted angles. Additionally, the ability to use bootstrap resampling makes this statistical approach favorable. Resampling was not done to provide an estimate of the distribution of the predicted values. The data retrieved from the GNSS-RF data packets and subsequent derivations provided us with the predicted value distribution. Rather, the bootstrap resampling is included to provide an estimate of the sampling distribution within the range of predicted angle measures; providing a larger sample size than could feasibly be obtained in fieldwork alone. The ability to increase sample size can strengthen the evidence for similarity in equivalence-based tests (Robinson et al. 2005).

All statistical analysis was performed in R (R Core Team 2016). The equiv.boot function in the "equivalence" package was used to evaluate equivalence tests (Robinson 2016). A total of 12 equivalence tests were conducted using 95% confidence intervals. These represented all combinations of the three transmission intervals (3), GNSS-RF transponder locations (2), and cycle elements (2). The equiv.boot function analyzes whether the slope and intercept of the regression of predicted angles fall within the desired region of equivalence, determining similarity or dissimilarity to observed angles. The region of equivalence for the regression was tested at +/−10% for both the slope and the intercept and 10,000 bootstrap replications were performed (Robinson et al. 2005). Equivalence testing shifts the burden of proof to difference.

2.4 Results

2.4.1 - Summary

Transmission interval ($p < 0.001$), transponder location ($p < 0.001$), and swing angle ($p < 0.001$) all affected the correct classification of cycle elements (Table 2.1 Chi-squared ANOVA table for parameter significance on correct classification proportion.). At the grapple, the proportion of verified correct classifications was greater for the 2.5 and 5.0 s transmission intervals than at the heel (Table 2.2). However, the proportion of correct classification for the 10.0 s interval was slightly higher at the heel than the associated grapple proportion. In all instances, the 2.5 s interval returned higher proportions of success than the other intervals, apart from the 5.0 s interval return element at the heel location. The proportion of correct classifications was least reliable overall for the 10.0 s interval, as expected, followed by the 5.0 s interval.

Table 2.1 Chi-squared ANOVA table for parameter significance on correct classification proportion.

Variable	Df [1]	Deviance	Resid. Df [2]	Resid. Dev. [3]	Pr (>Chi) [4]
NULL			2680	2054	
Interval	2	74.18	2678	1980	<0.001
Swing Angle	1	42.38	2677	1937	<0.001
Location	1	37.62	2676	1900	<0.001
Cycle Element	1	0.04	2675	1900	0.8421
Interval: Swing Angle	2	1.00	2673	1899	0.6043

[1] Degrees of freedom [2] Degrees of freedom of the residuals [3] Deviance of the residuals [4] P-value for the level of significance on correct classification

Only the 2.5 s interval was able to achieve greater than 90% classification success for a complete cycle and achieved 99% classification success for the Swing Unload element at the grapple location. The 5.0 s interval achieved 90% successful classification at the grapple location. The total swing angles for the duration of the trials captured by the transponders were underestimated. In this instance, the 2.5 s transponder returned the total angle for all 72 trials, and thereby best represented the actual swing totals.

Table 2.2 Summary data table.

Location	Interval	Element	Data Points	Total Angle (Degrees) Observed (GPS)	Proportion Correct
Grapple			1339		0.84 [1]
	2.5		769	27,360 (23,882)	0.94
		Swing Unload	451	13,680 (12,950)	0.99
		Return	318	13,680 (10,932)	0.88
	5.0		382	27,360 (21,442)	0.90
		Swing Unload	219	13,680 (11,698)	0.89
		Return	163	13,680 (9744)	0.91
	10.0		188	27,360 (14,918)	0.68
		Swing Unload	113	13,680 (8751)	0.71
		Return	75	13,680 (6167)	0.66
Heel			1342		0.79[1]
	2.5		773	27,360 (24,455)	0.82
		Swing Unload	443	13,680 (12,495)	0.84
		Return	330	13,680 (11,960)	0.80
	5.0		376	27,360 (22,740)	0.86
		Swing Unload	227	13,680 (12,609)	0.84

	Return	149	13,680 (10,131)	0.87
10.0		193	27,360 (15,558)	0.69
	Swing Unload	110	13,680 (9195)	0.71
	Return	83	13,680 (6363)	0.68

[1] Mean proportion of correctly classified elements across all treatments for Heel or Grapple location.

2.4.2 - Binomial Logistic Regression- Element Characterization

The odds of correctly classifying an element at the 10.0 s transmission interval was decreased 0.262 times when compared to the 2.5 s transmission interval, and was significant at a 95% confidence interval (CI) (Table 2.3).

Table 2.3 Logistic regression coefficients associated with model describing variable impact on whether GPS returned correct element classification as represented by field observations.

Variable	**Estimate**	**SE** [1]	***p*-Value**	**Odds Ratio**	**95% Confidence**
Intercept	1.748	0.212	<0.001	5.741	3.813–8.772
Rate 5	0.144	0.320	0.6525	1.155	0.621–2.182
Rate 10	−1.339	0.328	<0.001	0.262	0.138–0.499
Swing Angle	0.004	0.001	<0.001	1.004	1.003–1.006
Location Heel	−0.744	0.124	<0.001	0.476	0.372–0.605
Cycle Element	0.025	0.122	0.8374	1.025	0.807–1.300
Rate 5: Swing Angle	−0.001	0.002	0.3789	0.999	0.996–1.002
Rate 10: Swing Angle	0.000	0.002	0.8781	1.000	0.999–1.003

[1] Standard error of the variable estimate

The 5.0 s interval odds of correct classification was not significantly different than the 2.5 s interval. At each of the 18 observed angle intervals between 20 and 360, the odds of correct classification increased 1.004 times for each increasing interval with a CI exceeding 95%. In practice, this means that larger arcs have a higher incidence of correct classification. The location of the GPS transponders was also found to be a significant predictor (95% CI) of correct classification, with the odds of correct classification decreasing 0.476 times when moving from the grapple to the heel location. In practice, connected to arc distance, for the same arc in degrees, the heel moves a shorter distance than the grapple, resulting in more frequent misclassification. Observed element (Swing/Unload or Return) was not found to create differences in the odds of correct classification of cycle element.

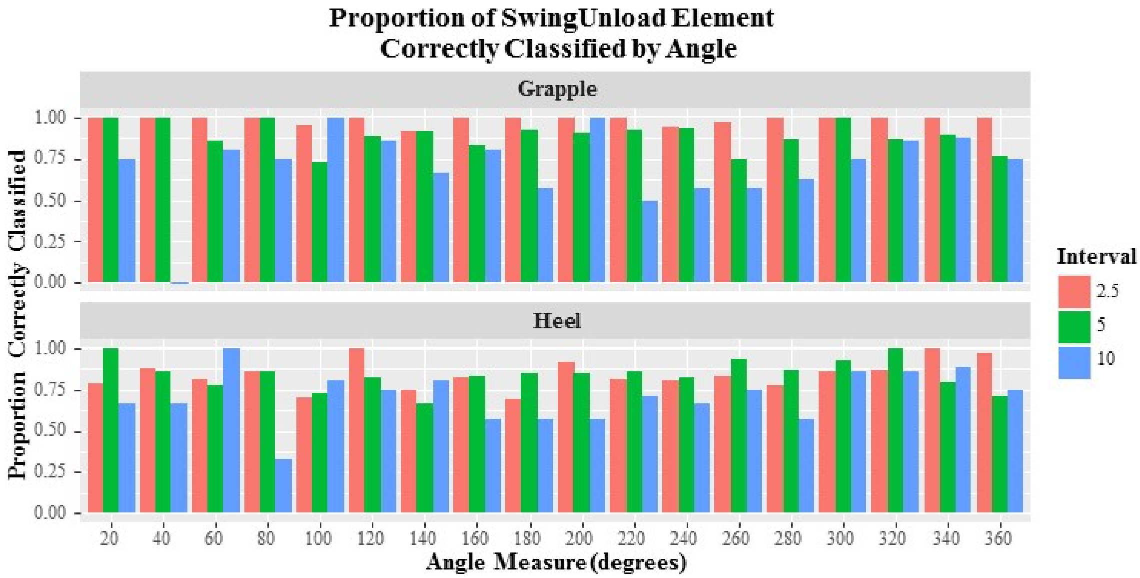

Figure 2.3 Bar chart representing the proportion of correct classifications of the Swing Unload cycle element at the grapple and heel locations at 18 angle intervals.

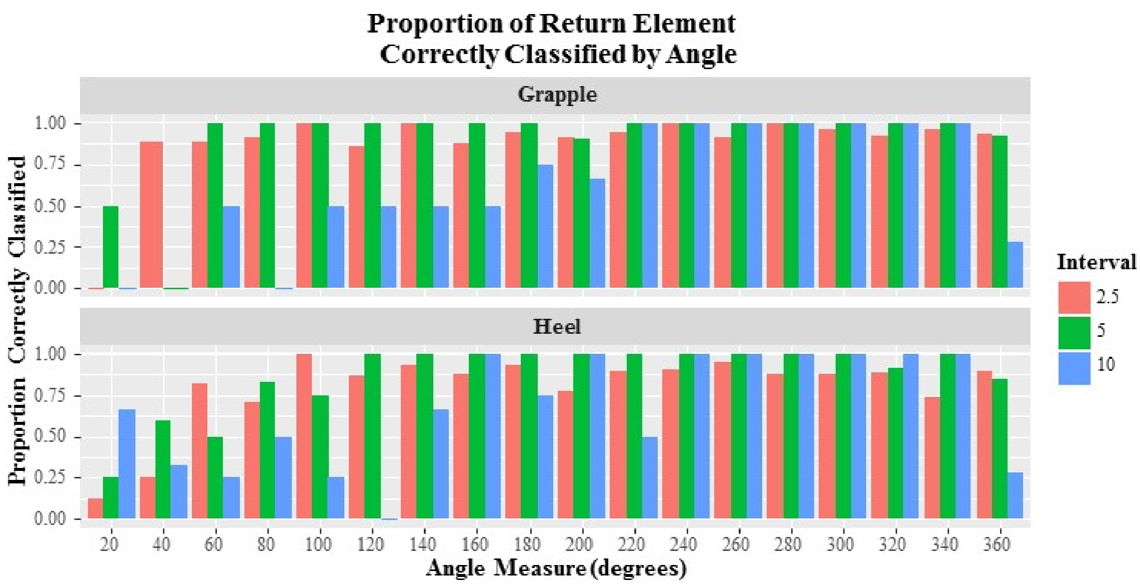

Figure 2.4 Bar chart representing the proportion of correct classifications of the Return cycle elements at the grapple and heel locations at 18 angle intervals.

2.4.3 - Swing Angle Analysis

Figure 2.5 shows a graphical comparison between the observed angle interval for each trial and the angles derived from GNSS-RF data packets for each transmission interval at both locations and for both elements. It is evident in the figure that the 2.5 and 5.0 s intervals most accurately capture overall angle measures at the grapple location, and that the heel location introduces greater error at both intervals. The solid black line in the figures represents a 1:1 relationship between the observed and the predicted values derived from the GNSS-RF recorded data packets. A clear trend of under prediction of swing angle can be seen in the figure for all transmission intervals, transponder locations, and machine elements. The most severe under-predictions are associated with the 10.0 s transmission interval, however. Both 2.5 and 5.0 s transmission intervals appeared to follow similar trends of underestimation in the predicted angles.

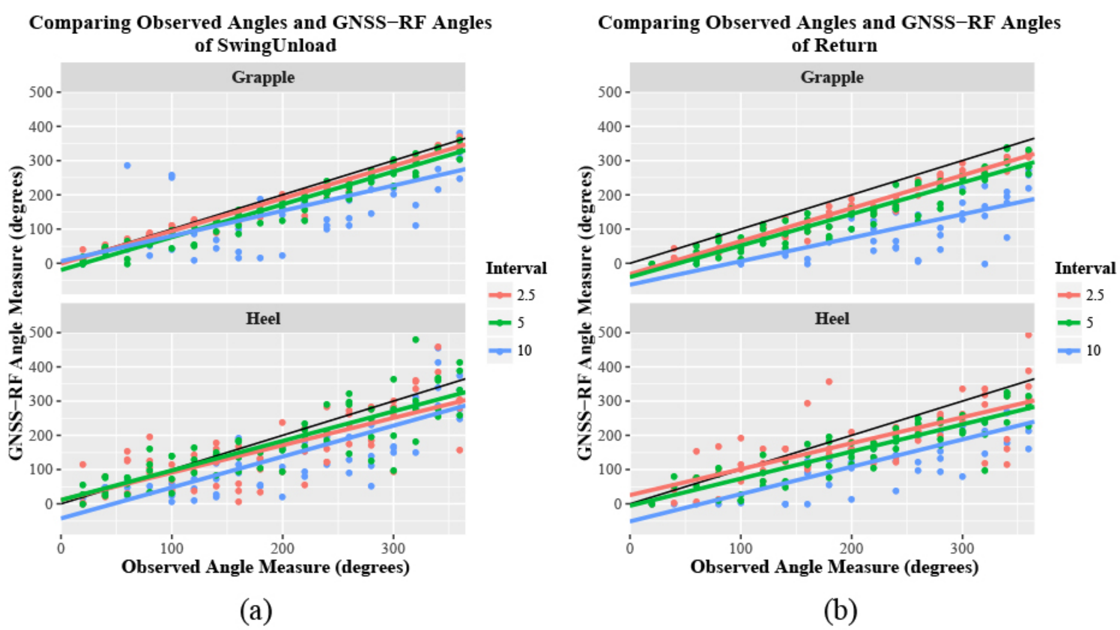

Figure 2.5 These figures represent the relationship between GNSS-RF derived angle measurements and observed angle intervals at the Grapple and Heel locations for the (a) Swing Unload and (b) Return elements.

Equivalence-based regression analysis showed that the only combination of GNSS-RF derived angles for which both the intercept and slope were statistically similar to the observed values was the transponder located at the grapple with a 2.5 s interval capturing the swing unload cycle element (Table 2.4). In all other instances the intercept was dissimilar for the predicted angle values when compared to the observed values. Only the 5.0 s interval swing unload element at the grapple and the 2.5 s interval at the grapple for the return element were found to be similar in regards to the slope of the regression line.

Table 2.4 Summary of equivalence-based regression results. The model represents the various combinations of transmission interval (2.5,5,10); transponder location, grapple (G) or heel (H); and cycle element, swing unload (SU), and return (R). Sample size is denoted by n, and the approximate joint two one-sided 95% confidence intervals for the slope and intercept are: ($C^{-}_{\beta_1}$, $C^{+}_{\beta_1}$) and ($C^{-}_{\beta_0}$, $C^{+}_{\beta_0}$), respectively. The former should be contained by the intercept interval of equivalence, ($I^{-}_{\beta_0}$, $I^{+}_{\beta_0}$) = $\bar{y}$ ± 25%, and the latter by the slope interval of equivalence ($I^{-}_{\beta_1}$, $I^{+}_{\beta_1}$) = 1 ± 0.25.

Model	n	$C^{-}_{\beta_0}$	$C^{+}_{\beta_0}$	$I^{-}_{\beta_0}$	$I^{+}_{\beta_0}$	β_0 Result	$C^{-}_{\beta_1}$	$C^{+}_{\beta_1}$	$I^{-}_{\beta_1}$	$I^{+}_{\beta_1}$	β_1 Result
G.SU.2.5	72	186.29	194.13	161.88	197.85	Reject	0.988	1.057	0.9	1.1	Reject
G.SU.5	72	184.46	195.91	146.23	178.72	Fail	0.934	1.042	0.9	1.1	Reject
G.SU.10	65	188.92	221.63	141.74	173.23	Fail	0.539	0.876	0.9	1.1	Fail
H.SU.2.5	72	175.16	205.88	156.19	190.90	Fail	0.533	0.779	0.9	1.1	Fail
H.SU.5	72	177.62	203.34	157.62	192.64	Fail	0.717	0.972	0.9	1.1	Fail
H.SU.10	64	192.70	220.46	129.30	158.04	Fail	0.625	0.893	0.9	1.1	Fail
G.R.2.5	68	195.02	205.03	144.68	176.83	Fail	0.946	1.035	0.9	1.1	Reject
G.R.5	66	196.55	212.46	132.87	162.40	Fail	0.886	1.044	0.9	1.1	Fail
G.R.10	44	229.89	263.50	95.75	117.03	Fail	0.468	0.902	0.9	1.1	Fail
H.R.2.5	67	187.15	218.16	160.66	196.36	Fail	0.603	0.920	0.9	1.1	Fail
H.R.5	63	199.18	221.60	144.72	176.88	Fail	0.864	1.097	0.9	1.1	Fail
H.R.10	48	216.13	245.22	119.30	145.81	Fail	0.699	1.022	0.9	1.1	Fail

The extent to which swing movements associated with each GNSS-RF transponder could be discerned visually varied with transmission interval (Figure 2.6). Visual interpretation of the tracks indicated that the 2.5 s transmission interval more accurately represented swing movements compared to 5.0 and 10.0 s transmission intervals. The data support this interpretation in that the angle totals best represented the actual swing angle totals for the 2.5 s interval. Higher frequency of data point collection creates a comparably smoother swing track than the 5.0 and 10.0 s transmission intervals. The movements of the cab during the experiment were also captured by an additional transponder located on the rear corner of the cab. The transponders located at the grapple and heel remained equidistance from the cab transponder throughout the duration of the experiment.

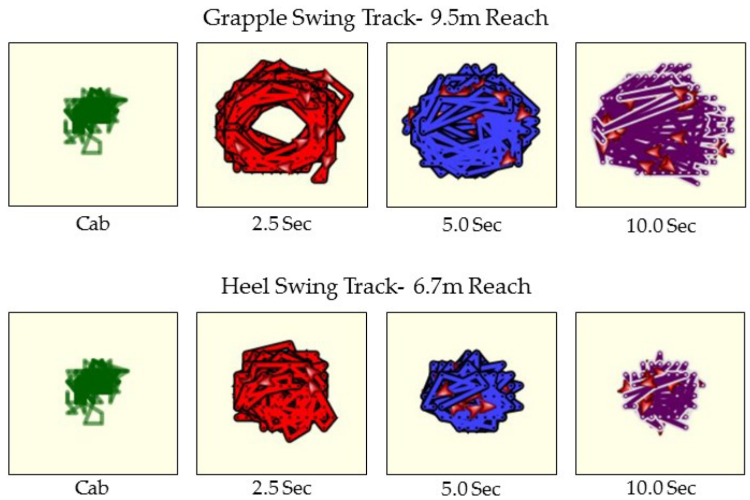

Figure 2.6 The GNSS-RF transponders create a movement progression track between data points through the duration of the trials which are shown for the two (2) transponder locations and three (3) transmission intervals used in the experiment in addition to the cab location.

2.5 Discussion

Analysis of the field data returned both expected and surprising results. As anticipated, the 2.5 s transmission interval data returned the highest proportion of correct element classifications. However, the 5.0 s transmission interval returned comparable correctly classified proportions. With 2.5 and 5.0 s transmission intervals capturing 94.4% and 91.7% of the respective overall cycles with at least one correct element for both Swing Unload and Return at the Grapple, accuracy exceeding that described by McDonald and Fulton (2005) and similar to that described by Hejazian et al. (2013) was obtained when classifying machine cycles using GNSS data. The ability to correctly classify at least one observation of each element within each trial was reduced when analyzing the Heel data. The associated percentages of success for the 2.5, 5.0, and 10.0 s intervals at the Heel were 91.7%, 88.9%, and 58.3%, respectively. Even so, if, for some operational reason, the transponders were placed at the heel rather than the grapple, a transmission interval of 2.5 or even 5.0 s would provide useful data, depending on accuracy requirements.

When addressing the potential for GNSS-RF transponders to accurately capture angle measurements, a consistent trend of angle underestimation was found across all angles exceeding 180 degrees, though at the smaller angle measures this underestimation is decreased and in some cases there is predicted angle overestimation (Figure 2.5). The reason for this underestimation at the larger observed angle measures is likely due to transponder data packets representing the machine swing not capturing the full extent of the swing arc. For the GNSS location to represent the true arc angle, the transponder has to record a data packet the exact moment the full swing extent is reached or during any pause at the full extent. The time of a pause at full extent is a greater proportion of the overall time at shorter arcs, resulting in a higher inclusion probability of a data packet representing full swing extent. Therefore, the full extent would be represented more often for smaller swing angles and would result in lower underestimation of swing angles. As seen in Figure 2.5, any intersection of the 1:1 line and the time interval trend line represents a location where the predicted angles derived from the GNSS-RF data match observed angles. Additionally, Figure 2.5 and Table 2.4 indicate overall that the 2.5 s interval is most successful in capturing data to derive accurate angle measures.

In our analysis, there was a trend of decreased GNSS measurement accuracy at the Heel location when compared to the Grapple location. The movement of the transponders around a smaller swing circumference means the transponders are less likely to be able to accurately and concisely plot varying points because the range of the movements is shorter. This is due to the inherent accuracy of GNSS. For example, GNSS accuracy of +/− 1 m will have a greater impact on accurately capturing movements when the overall distance traveled 5 m as opposed to 15 m or 20 m. One possible solution to help account for this error when the swing arc is smaller is to incorporate additional sensors and mechanisms to capture grapple and other intricate movements to assist in defining elements (Palander et al. 2013). These would augment GNSS data in ways that get around constraints related to GNSS accuracy. At the longer GNSS-RF transmission intervals, minute machine boom movements are not as accurately captured. This is seen by observing both the positional data itself, as well as the successful classification proportions. This is especially clear for the 10.0 s interval data. As suggested by Devlin and McDonnell, the 10.0 s interval may be beneficial for analysis of general machine movements across the landscape (Devlin and McDonnell 2009). However, precise and intricate machine movements are best captured and analyzed using higher frequency data transmission of locations. Importantly, transmission intervals should be tested and tailored to meet the needs of particular equipment movements rather than relying on a general rule of thumb.

From a visual representation standpoint, it is evident in Figure 2.6 that the 2.5 s transmission interval results in a plotted machine movement track that has smoother curves and higher accuracy representation of precise machine movements and machine component locations to meet operational analysis objectives. Correct classification of elements and overall cycles exceeding 90% for the 2.5 s interval further support this observation, as does the results of the regression based equivalence test. However, higher frequency transponder transmission rates are also more data intensive, requiring twice the data flow and storage capacity. This intensity could be difficult to manage for large projects with many pieces of equipment, both in terms of data collection and storage, but also real-time analysis, validation, and model optimization. When addressing the ability of the transponder to accurately characterize machine cycles, cycle elements, and angles of swing, the 5.0 s interval was shown to return comparable accuracies to those obtained by the 2.5 s interval transponders, at half the data intensity.

In this particular study, the overall sampled time represented only a small portion of what a full productive work day would entail in a commercial logging operation in beetle-killed timber. With the 2.5 s interval, the available storage space needed for each data file will be utilized twice as fast as the 5.0 s interval. Each file saved can consist of up to 9999 data points, after which the device overwrites existing data by default. Therefore, a new file needs to be saved on the handheld receiver every 6.9 h when working with the 2.5 s transmission interval to avoid overwriting and every 13.8 h when working with the 5.0 s transmission interval with three transponders. If additional transponders are used on multiple pieces of equipment, then available storage space will be used up more quickly. This can present problems with data being overwritten during average work days if the file is not saved, e.g., mid-way through the day. Additionally, it was found that the large data pools associated with the 2.5 s interval made analysis and interpretation of the data more cumbersome and time intensive than the longer intervals, an observation also made by de Hoop and Duprè (2006). Depending on the specific application, machines, and desired level of accuracy, incorporating the 5.0 s interval could return acceptable, though slightly lower, accuracies than the 2.5 s interval. In turn, longer work cycles could be sampled without concern for overwriting data and analysis and interpretation of those data would prove quicker and easier than with the 2.5 s interval if available memory storage and analytical capacity is a concern. When interest is focused on positioning and analysis of precise machine movements where rapid machine movements may be missed by long transmission intervals, the 2.5 s interval likely provides the best option for transmission frequency, or perhaps the study requires more traditional work study methods that relies on direct rather than passive observation.

An important consideration with our study is that the Garmin Alpha receiver and positioning transponders were located in open line-of-sight conditions, which may not be typical of many forest stands. No transmissions were obstructed by vegetation, topography, or inter-machine positioning. One hundred percent of the time-stamped positional coordinates were received. Prior experience with GNSS-RF data in operational forestry has shown that GNSS position and radio signal propagation quality (RSSI) can interact in complex ways. In operational forestry, there are many situations in which positioning transponders may receive a GNSS signal (Keefe et al. 2014a; Grayson et al. 2016), but radio propagation of coordinates to other devices elsewhere on the jobsite is blocked topographically by dense vegetation or interference from other radio systems (Keefe et al. 2014a; Grayson et al. 2016). If a portion of data packets are missing due to radio signal interference, the classification of machine elements may be affected in more complex ways not evident in our controlled experiment. With the quantities of data collected in this way, post-hoc manual and visual inspections of outlier points is almost impossible, so automated data quality control procedures are especially critical in such an environment.

In order to further develop real-time modeling of machine movements on active logging operations, further studies exploring the impacts of forest canopy on GNSS-RF accuracy in particular applications should be explored. For example, in stands with high mortality due to beetle-kill with many trees that have dropped most of their foliage, this may not be a problem, but that remains to be evaluated. Past studies exploring canopy impact in GNSS accuracy have shown large decreases in accuracy depending on canopy cover (Sigrist et al. 1999; Taylor et al. 2001; Veal et al. 2001; Yoshimura and Hasegawa 2003; Bolstad et al. 2005; Hasegawa and Yoshimura 2007; Devlin and McDonnell 2009). However, these studies were for GNSS only and did not study dual effects of canopy on GNSS and RF, or the interaction of these two signals. Because canopy density tends to be low in beetle impacted stands due to high levels of mortality, for example, canopy impacts on GNSS multipath error may be less of a concern than in healthy stands. Additionally, developing a methodology for similar element and cycle classification when the machine is traversing the landscape on steep slopes in beetle impacted stands in biomass utilization operations as opposed to sitting in a fixed location on flat ground will be necessary. Introducing machine movements on slopes into the analysis will add an additional level of complexity but is important for development of subsequent applications to improve the efficiency of harvesting in beetle impacted and unaffected forests alike.

2.6 Conclusions

Both 2.5 and 5.0 s transmission intervals correctly characterized cycles and cycle elements in the rotation movements of log loaders. However, the 2.5 s interval was the most successful in allowing for the prediction of accurate swing angle measures. Additional studies should be conducted to further refine the methodology and analysis techniques to foster use of this approach in real-time analysis of equipment movements on active beetle-killed harvesting operations. Accurate characterization of machine movements from spatially explicit data through the use of simple, non-intrusive multi-transmitter GNSS-RF allows for an increased level of situational awareness for improved streamlined operational production in the woods where obstructed views from topography or other site features may limit the ability to visually identify the actions of forest machinery at all times. The consumer-grade transponders incorporated into this study returned promising results in this preliminary study as to their accuracy and use in real-time production analysis and support models. The designed and controlled experiment performed in this study provided valuable information which will be used to further develop the real-time analysis model in subsequent studies. Executing these focused studies will allow various machine processes to be analyzed individually, resulting in strong model components representing the various cycle elements of associated harvest machinery. As previously mentioned, once activity profiles for harvest systems are completed, the model will be applied at a landscape scale, providing valuable information to operations foresters and contractors regarding harvest site selection and real-time decision support during harvest.

Further, connecting machine movements to the onboard computers of multiple machines interacting with one another opens new possibilities for real-time decision-support and logistics analysis in beetle-killed harvests and forest operations in general. For example, the movements of a shovel can be paired with subsequent processing activities of additional machinery and personnel working within the harvest boundaries. Incorporation of real-time machine production analysis and model-assisted decision-making will prove a valuable development in the continued advancement of precision forestry. These technologies will allow for streamlined real-time production analysis and feedstock logistics in not only beetle-killed harvests, but more broadly in a wide range of forest operations.

2.7 References

Anderson N, Chung W, Loeffler D, Jones JG. 2012. A productivity and cost comparison of two systems for producing biomass fuel from roadside forest treatment residues. For Prod J. 62:222–233.

Anderson N, Mitchell D. 2016. Forest operations and woody biomass logistics to improve efficiency, value and sustainability. Bioenerg Res. 9:518–533.

Bolstad P, Jenks A, Berkin J, Horne K. 2005. A comparison of autonomous, WAAS, real-time, and post-processed global positioning systems (GPS) accuracies in northern forests. North J Appl For. 22:5–11.

Brown RT, Agee J, Franklin J. 2004. Forest restoration and fire: Principles in the context of place. Conserv Biol. 18: 903–912.

Carter EA, McDonald TP, Torbert JL. 1999. Application of GPS technology to monitor traffic intensity and soil impacts in a forest harvest operation. Proceedings of the Tenth Biennial Southern Silvicultural Research Conference; February 16-18; Shreveport, LA.

Danskin SD, Bettinger P, Jordan TR, Cieszewski C. 2009. A comparison of GPS performance in a southern hardwood forest: Exploring low-cost solutions for forestry applications. South J App For. 33:9–16.

de Hoop CF, Duprè RH. 2006. Using GPS to document skidder motions: A comparison with manual data collection. Proceedings of the Council on Forest Engineering (COFE): Working Globally- Sharing Forest Engineering Challenges and Technologies Around the World; July 22-August 2; Coeur d’Alene, ID.

Devlin GJ, McDonnell K. 2009. Performance accuracy of real-time GPS asset tracking systems for timber haulage trucks travelling on both internal forest road and public road networks. Int. J. For. Eng. 20:45–49.

Grayson LM, Keefe RF, Tinkman WT, Eitel JUH, Saralecos JD, Smith AMS, Zimbelman EG. 2016. Accuracy of WAAS-Enabled GPS-RF warning signals when crossing a terrestrial geofence. Sensors. 16:1–8.

Hamzah KA. 2001. Remote sensing, GIS and GPS as a tool to support precision forestry practices in Malaysia. In Proceedings of the 22nd Asian Conference on Remote Sensing; November 5-9; Singapore.

Hasegawa H, Yoshimura T. 2007. Estimation of GPS positional accuracy under different forest conditions using signal interruption probability. J For Res. 12:1–7.

Hejazian M, Hosseini S, Loftalian M, Ahmadikoolaei P. 2013. Possibility of global positioning system (GPS) application for time studies in forest machinery. Euro J Exp Bio. 3(4):93-98.

Jacobson RA, Keefe RF, Smith AMS, Metlen S, Saul D, Newman SM, Laninga TJ, Inman D. 2016. Multi-spatial analysis of forest residue utilization for bioenergy. Biofuels Bioprod Bioref. 10:560–575.

Keefe R, Anderson N, Hogland J, Muhlenfeld K. 2014. Woody biomass logistics. In: Karlen DL, editor. Cellulosic energy cropping systems. Hoboken (NJ): John Wiley & Sons. p. 251–278.

Keefe RF, Eitel JUH, Smith AMS, Tinkham WT. 2014. Applications of multi-transmitter GPS-VhF in forest operations. Proceedings of the 47th International Symposium on Forestry Mechanization and 5th International Forest Engineering Conference; September 23-26; Gerardmer, France.

McDonald TP, Fulton JP. 2005. Automated time study of skidders using global positioning system data. Comput. Elec Ag. 48:19–37.

NIST Internet Time Servers. 2016. Boulder (CO): National Institute of Standards and Technology; [accessed 2016 May 15]. http://tf.nist.gov/tf-cgi/servers.cgi.

Palander T, Nuutinen Y, Kariniemi A, Vaatainen K. 2013. Automatic time study method for recording work phase times of timber harvesting. For Sci. 59:472–483.

R: A language and environment for statistical computing. 2016. Vienna(Austria): R Foundation for Statistical Computing R Core Team; [accessed 2016 September 10]. https://www.R-project.org/.

Robinson AP, Duursma RA, Marshall JD. 2005. A regression-based equivalence test for model validation: Shifting the burden of proof. Tree Physiol. 25:903–913.

Robinson AP, Froese RE. 2004. Model validation using equivalence tests. Ecol Model. 176:349–358.

Robinson AP. Equivalence: Provides Tests and Graphics for Assessing Tests of Equivalence; R package version 0.7.2., Melbourne, Australia, 2016; Available online: https://CRAN.R-project.org/package=equivalence (accessed on 17 October 2016).

Rummer B, Prestemon J, May D, Miles P, Vissage J, McRoberts R, Liknes G, Shepperd WD, Ferguson D, Elliot W. et al. 2003. A strategic assessment of forest biomass and fuel reduction treatments in Western states. Fort Collins (CO): USDA Forest Service Rocky Mountain Research Station. Report No.: RMRS-GTR-149.

Sigrist P, Coppin P, Hermy M. 1999. Impact of forest canopy on quality and accuracy of GPS measurements. Int J Remote Sens. 20:3595–3610.

Strandgard M, Mitchell R. 2015. Automated time study of forwarders using GPS and a vibration sensor. Croatian J For Eng. 36:175–184.

Strandgard M, Walsh D, Acuna M. 2013. Estimating harvester productivity in Pinus radiata plantations using StanForD stem files. Scan J For Res. 28:73–80.

Taylor SE, McDonald TP, Veal MW, Grift TE. 2001. Using GPS to evaluate productivity and performance of forest machine systems. Proceedings of the First International Precision Forestry Symposium; June 20-21; Seattle, WA.

Veal MW, Taylor SE, McDonald TP, McLemore DK, Dunn MR. 2001. Accuracy of tracking forest machines with GPS. Trans American Soc Ag Eng. 44:1903–1911.

Wang J, McNeel J, Baumgras J. 2003. A computer-based time study system for timber harvesting operations. For Prod J. 53:47–53.

Wells L, Chung W, Anderson N, Hogland J. 2015. Estimating bioenergy feedstock supply and delivered costs. Proceedings of the Council on Forest Engineering (COFE): Engineering Solutions for Non-Industrial Private Forest Operations; July 19-22; Lexington, KY.

Wing MG, Eklund A, Kellogg LD. 2005. Consumer-grade global positioning system (GPS) accuracy and reliability. J For. 103:169–173.

Yoshimura T, Hasegawa H. 2003. Comparing the precision and accuracy of GPS positioning in forested areas. J For Res. 8:147–152.

Chapter 3: Use of LiDAR-derived landscape parameters to characterize alternative harvest system options in the Inland Northwest

3.1 Abstract

As new, innovative harvest options become available, it's often unclear to forest managers how much area may potentially be available for those alternative harvest system options. Spatial decision support models can aid contractors and forest planners in choosing appropriate harvest systems based on topography and stand characteristics. In this study, high resolution, remotely sensed LiDAR data and inventoried stands characteristics from 91 sample plots were used to model landscape scale stand characteristics for the Slate Creek drainage on the Nez Perce Clearwater National Forest in North-Central Idaho. Raster layers for stand density and volume were overlaid onto high resolution digital elevation model and then integrated into a decision support model to compare harvest system selection within three scenarios composed of five harvest systems. In each subsequent scenario, shovel harvester based harvest systems were included to determine potential sites where integration of new harvest systems may be beneficial. Harvest system classification using LiDAR-derived products when introducing alternative harvest systems allows contractors and managers to better evaluate the operable capabilities of alternative harvest system options on landscape scales. This may additionally encourage the utilization of innovative machinery not currently widely integrated into logging operations.

3.2 Introduction

Harvesting system selection in forest operations is an integral component of applied forest management. Forest stands vary greatly in tree height, diameter, volume and topographic characteristics, resulting in a need for forest managers to effectively and efficiently select harvest systems best equipped to handle these varying conditions (Wang et al. 1998; Adams et al. 2003). Decades of forest operations research and industrial timber harvesting experience has led to general understanding of the capabilities and operational thresholds of existing logging systems. However, as technology advances and equipment evolves over time, the tool box of available harvest systems from which to choose continues to grow, making it necessary for managers and contractors to stay informed about innovation in harvest systems (Kuhmaier and Stampfer 2010) and to better understand the trade-offs among conventional and emerging options, and the potential landscape area for which newer options may be preferable. The choice of harvesting system has large impacts on costs, and machine and workforce capacity (Matthews 1942; Kuhmaier and Stampfer 2010). Incorporating this knowledge and understanding into the context of precision forestry, aimed at site-specific forest management decision making and operations, provides a valuable resource for long-term sustainability, improved logging production and environmental quality protection.

Broken or irregular topography creates unique challenges in harvest system selection and planning that are largely driven by fine-resolution spatial patterns (Saralecos et al. 2014; Saralecos et al. 2015). These factors make operations in sensitive and steep terrain more complex than gentle terrain operations (Abbas et al. 2017). In addition, natural resource management is facing greater demand to meet sustainability certification standards (Laukkanen et al. 2005). This is especially relevant in the Inland Northwest where lower bulk densities, high porosity, weaker structural development and lower cohesion of an ash-cap layer makes soils highly susceptible to compaction and disturbance that can limit future site growth potential (Page-Dumroese 1993; Johnson et al. 2005). The US Forest service restricts skidding on ground exceeding 35% to reduce soil disturbance, with other landowners across Idaho and

US employing similar restrictions (Greulich et al. 2001; D. Hollenkamp, personal communication, 2014; Barkley et al. 2015). However, low-impact, self-leveling machines may result in exceptions to existing restrictions if they are shown to operate below desired soil disturbance criteria.

Working on steep slopes presents challenges associated with worker safety and logging production due to challenging terrain and less than ideal working conditions (Amishev and Evanson 2010). Ground based systems are generally associated with higher production and lower costs, as compared to cable systems (Andersson and Young 1998; Strandgard et al. 2014). This makes tethered, or cable-assist steep slope harvesting systems an appealing alternative to cable systems within feasible operational thresholds. Tethered systems may improve logging safety by reducing the number of ground workers and allowing workers to operate from the safety of a protected machine cab (Abbas et al. 2017). For example, the hazards associated with motor-manual felling can be mitigated by performing felling operations, where feasible, with a fully-mechanized option. Additionally, self-leveling chassis of harvesting machines designed for steep slopes increases the safety, comfort of operation, and sustained high efficiencies on steep terrain when compared to fixed cab ground based machines (Gellerstedt 1998, MacDonald 1999; Acuna et al. 2011). Self-leveling shovel harvesters both fell and forward trees to the roadside, fulfilling the harvest tasks of two separate machines and decreasing the number of machines on the job site. Areas traditionally harvested using a feller-buncher and grapple skidder system can be harvested and forwarded to the roadside using a single machine. Even though it is unlikely that the single shovel harvester would be able to match the production of two machines working simultaneously, lower delay and idle times for a single machine may result in lower unit production costs.

Along with increased use of self-leveling shovel logging units in the Inland Northwest, contractors have also started incorporating tethered harvest systems into steep slope operations. With early work exploring tethered systems beginning in the early 1970's, tethered forestry equipment has since become commercially available and has been so in Europe for over 15 years (McKenzie and Richardson 1978; Visser and Stampfer 2015; Sessions et al. 2017). Over the past 5 years, New Zealand has seen a huge increase in the popularity of winch-assist technology, with over 50 units actively operating (Abbas 2017). There are now over 45 winch-assisted machines operating in North America as well; 23 of which are in the Pacific Northwest (Amishev 2017). These include systems incorporating either a dedicated winch machine or an integrated winch mechanism on the harvester (Amishev and Evanson 2010; Visser and Stampfer 2015; Sessions et al. 2017). As use of tethered logging systems increases, so does the importance of efficiently and effectively characterizing feasible logging system alternatives at the harvest unit and landscape scales.

Decision support systems are defined as any means or tools used to aid in decision making processes (Acosta and Corral 2017). In forest operations research, decision support is often utilized to define machine activity and harvest system classification. Past research has resulted in the development of various decision support systems for harvesting type selection based on terrain and site characteristics (Reisinger and Davis 1986; Davis and Reisinger 1990; Hartsough et al. 2001; Suvien 2006; Kuhmaier and Stampfer 2010). In the context of steep, mountainous operations, various tools have been developed and have been applied operationally in varying levels (Heinmann 1998; Stampfer et al. 2001; Chung et al. 2004; Largo et al. 2004; Acuna et al. 2011; Bell and Keefe 2014; Barger et al. 2015; Bell et al. 2017).

Development of a harvest system selection and decision support model that effectively facilitates alternative logging system analysis on the broken topography of the Inland Northwest region is challenging (Moye et al. 1988). Increased application of self-leveling shovel systems and tether-matched harvest systems creates a need for a descriptive harvesting classification. Quantifying trade-offs among alternative, feasible harvest system options based on site and stand characteristics could aid land managers in decision making processes and help improve the operational efficiency of operational planning. Quantifying topographic and forest metrics for management areas is an important first step in this process.

Remotely sensed data, including lidar (light detection and ranging), has been used widely in forest management and research (Akay et al. 2009). Advancements in the availability of lidar and associated data processing capabilities provides opportunities to further develop decision support tools with high spatial resolution. Stand metrics and topographic products derived from lidar also facilitate the extrapolation of such models to a landscape scale (Reutebuch et al. 2005). Inventoried forest plots and the subsequent development of predictive models using random forest classification and regression methods with lidar data allows stand metrics including trees per acre, merchantable volume and basal area to be processed for landscape scale analyses (Breiman 2001; Rodriguez-Galiano et al. 2012; Gan et al. 2015; Hudak et al. 2016). Topographic and site variables can be predicted and processed at resolutions as fine as 1 meter (Reutebuch et al. 2005). The resultant products from lidar provides unique opportunities to further advance the field of precision forestry and the degree to which decision support models influence land management strategies.

While lidar has been widely used in forest inventory analysis, the utilization of these data in the context of forest operations has not be widely explored. In forest operations, research utilizing lidar has focused primarily on its use for developing high resolution digital elevation models (DEMs) for forest road layout (Akay et al. 2004; Aruga et al. 2005; Akay and Sessions 2005; Akay et al. 2009; Alam et al. 2013). For example, Alam et al. (2013) incorporated lidar-derived slope data for a simulation model of a self-leveling feller-buncher. Our goal in this paper was to develop a simple decision support model using lidar-derived forest and topographic metrics for broad-level harvest system selection at the landscape scale, to determine where innovative, alternative harvest systems such as self-leveling shovel logging and tether-matched steep slope harvest systems are feasible alternatives to conventional logging systems.

We determined the impact that introducing alternative ground-based harvest systems using shovel logging and tether-matched systems had on the classification of stands when compared to other commonly used ground and cable based operations. This was done by testing three harvest system scenarios, with each subsequent scenario introducing an additional harvest system to the previous scenarios. The first scenario explored the use of three harvest systems, followed by four and five systems in the following two scenarios. We hypothesized that the area of land classified as feller-buncher and skidder would change significantly when introducing the ground based shovel harvester as an alternative logging system moving from the first to second harvest system classification. Additionally, we hypothesized that the introduction of a tethered shovel harvester system would have a significant impact on the land previously classified as excaliner and hand fell in our harvest system classification across the study area in classifications 2 and 3. For all three scenarios we included a variant A and B to explore the impact of increasing operable slope for ground-based systems on overall harvest system classification. We expected lidar-derived products to provide the needed forest and topographic metrics to perform landscape scale harvest system classification and provide the foundational data necessary for subsequent production and cost analyses in the future.

3.3 Methods

3.3.1 - Methods Overview and Study Site

We developed a process for harvest system site classification based upon forest and topographic characteristics for 5 harvest systems within three varying harvest scenarios. This provides an opportunity for operations managers and harvest planners to be able to perform direct comparisons between the harvest systems to aid in the selection of feasible harvest systems based on the stand characteristics, terrain and machine parameters. The model classifies stands within the management area based on forest and topographic characteristics including stand stocking, merchantable volume, site slope, aspect and harvest unit dimensions. The study area is northeast of Riggins, Idaho in the Nez Perce Clearwater National Forest and consists of over 30,000 hectares (74,000 acres) with 2,627 delineated stands of mixed-conifer over story. Stands were previously delineated by the USDA Nez-Perce Clearwater National forest and the spatial data was provided upon request to assist in analysis. Mountain pine beetle (Dendroctonus ponderosae) has resulted in mortality across the management area, resulting in salvage focused harvests in addition to other active harvests and fuel treatments. In most cases, these harvests consisted of clearcut salvage harvests, though mastication has been used in some instances to change fuel composition and structure in affected stands.

3.3.2 - Lidar-derived Stand Metrics

To quickly generate stand stocking reports for vast areas, traditional inventory methods for collecting stand data was replaced with analysis using lidar data. Data from 91, 405 square meter inventory plots were input into the forest vegetation simulator (FVS) to develop inventory summary tables for stand composition and structure. Only trees greater than and equal to the 15-centimeter diameter class were considered for further use in data processing to represent only potentially merchantable trees. Lidar metrics encompassing the same extent as the inventory plots were also acquired. This data allowed the development of random forest models aimed at determining the relationship between the inventory metrics in question (trees per hectare, basal area, and merchantable volume) and the corresponding lidar metrics for the plots.

A random forest is an ensemble learning technique that combines multiple decision trees into an overall ensemble to provide a much stronger approximation of the underlying data. This process is comparable to a form of nearest neighbor approximation which incorporates a bootstrapping algorithm with decision trees. While predictions from a random forest are limited to the range of the training data in regression, they are run quickly and are very capable of dealing with unbalanced and missing data (Breiman 2001). The rapid processing capabilities and robustness of the ensemble learning method, despite potential missing values, were the primary factors in choosing random forests. Three separate random forest models were built using the randomForest package (Liaw and Wiener 2002) in the data processing environment, R version 3.3.3 (R Core Team 2016). Additionally, the rfUtilities package (Evans 2017) was used to optimize predictor variable selection during model development.

After random forest models were built for trees per hectare, merchantable volume and basal area, they were then applied to the overall Slate Creek study area. Lidar data were acquired through the Idaho Lidar Consortium and represented 217 separate .las point cloud files from a single 2006 lidar flight acquisition. These files were processed using the USDA lidar processing and analysis software, FUSION version 3.60. An identical lidar post-processed data structure to those of the 91 existing training plots were developed to allow the random forest models built from the 2/3rd training data and later validated using the remaining 1/3rd test data set to be applied directly to the entire study area. Basal area, merchantable volume and trees per hectare rasters in 405 square meter resolution were predicted.

Shapefiles representing the delineated stands for the entire study area were used to create boundaries for the application of the harvest system selection model. The raster files for the complete study area where then split and delineated to the extent of each of the 2,627 stand shapefiles. Average values for stand slope, trees per hectare, basal area (m2/ha), and merchantable volume (m3/ha) were determined for each of the 2,627 stands using the lidar derived 405 square meter stand and slope metrics. Stands level averages for the forest and site metrics (merchantable volume, stocking density, basal area, slope, and aspect) were then determined across the study area. All lidar-derived and additional spatial data sources incorporated into the study analysis and interpretation are referenced in Figure 1.

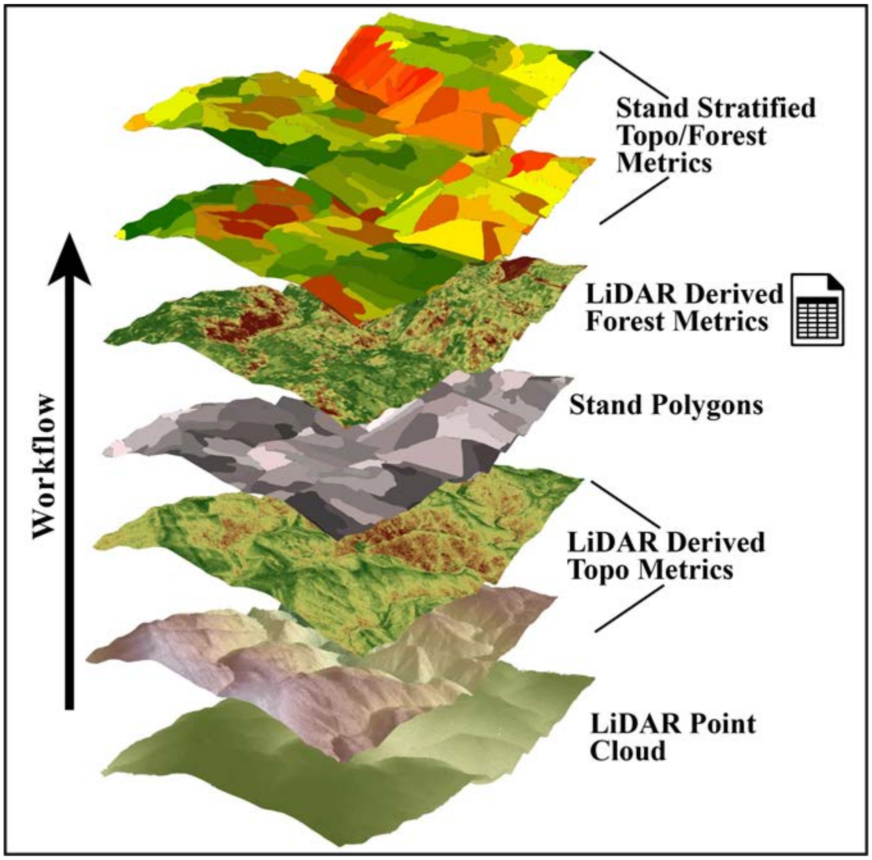

Figure 3.1 Multi-tiered spatial data sources for harvest system selection model

3.3.3 - Harvest System Classifications and Forest and Topographic Metric Classifications

Three landscape scale harvest system scenarios were addressed through the analysis process, representing the implementation of 5 varying harvest systems across the Slate Creek study area in different combinations (Figure 2).

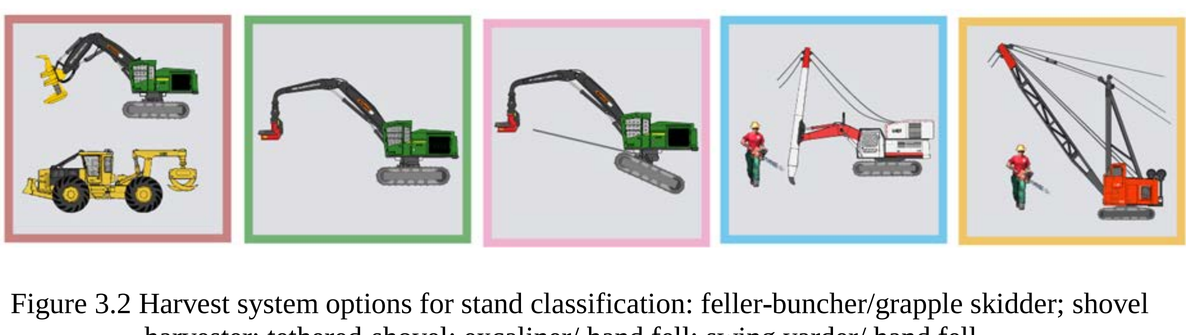

Figure 3.2 Harvest system options for stand classification: feller-buncher/grapple skidder; shovel harvester; tethered-shovel; excaliner/ hand fell; swing yarder/ hand fell

Performing landscape scale queries of stand and site characteristics for various combinations of harvest equipment provided insight into the way in which new harvest system introduction across the landscape impacted the distribution and area of feasible harvestable land for each system described. Three harvest systems remained constant in the three scenarios: feller-buncher with wheeled skidder; hand felling with excaliner skid; and hand felling with swing yarder skid. In the second scenario, a shovel harvester system, which includes felling and forwarding with a single machine, was included in the analysis. The operational threshold of the shovel harvester overlapped with that of the feller-buncher and wheeled skidder system. However, the shovel harvester was the preferred system when performing the harvest system selection query across the 2,627study area stands. The ability to operate one machine, the shovel harvester, as opposed to the skidder and feller-buncher, may lead have some operational and cost benefits. Therefore, giving classification priority to the shovel harvester gives insight into area where these benefits have the potential to be captured.

In the third scenario, the four harvest systems previously referenced in the second scenario were incorporated once again. Additionally, a tethered shovel harvester system was included in the analysis. Any instances where the operational threshold of the tethered shovel harvester system overlapped existing harvest systems' operational thresholds, the tethered system was used as the preferred system. Again, this classification priority given to the tethered shovel was to determine the areas where the tethered shovel is a feasible alternative to the excaliner and where incorporating the ground based system may yield beneficial returns. Higher production and lower costs of ground based harvesting systems as opposed to cable counterparts is the justification behind this analysis process.

Analysing harvest systems and identifying limiting parameters within harvest systems has previously been successfully described by decision support models using systems analysis (Talbot et al. 2003). To delineate the stands in each scenario by each harvest system, operational thresholds were defined for each of the systems and were the foundation for the classification process. Operational thresholds for slope, forwarding/skid distance and minimum merchantable volume were defined for all systems (Table 1). The shovel harvester harvest system independent of other machinery is limited to forwarding distances not exceeding 180 meters (Krume, personal communication 2015; Fisher 1999). Forwarding distance for the manual felling with excaliner yarding systems is restricted to distances not exceeding 250 meters. Any stand with a slope exceeding 35 percent and forwarding distance exceeding 250 meters in variant A was consistently classified across all three scenarios as hand fell and swing yarder skid. This slope was increased to 45 percent in variant B. In all three scenarios, stands not exceeding 35 percent slope and exceeding 180-meter forwarding/skidding distance were classified as feller-buncher and wheeled skidder in variant A. This lower slope limit was increased to 45 percent in variant B. This was similarly the case in scenario 1 for stands below 180-meter forwarding/skidding distance.

The tethered shovel-harvester system was bound by the same operational thresholds has the untethered shovel harvester apart from the allowable operable slope. In this instance, the operable slope began at 35 percent in variant A and 45 percent in variant B and was restricted to a maximum of 85 percent (Cavalli 2015). For each of the previously described harvest system scenarios, operational thresholds for slope and maximum skidding/forwarding distance are shown in Table 1. In all instances, the minimum merchantable volume for classified stands exceeded 29 m3/ha (5,000 BF/acre). Any stand with mean volume below this minimum bound was excluded from harvest system classification due to the infeasibility of performing a harvest in a stand with such low merchantable volume. These operational threshold benchmarks defined are flexible estimates and are used to present the methodology used in this paper. Any limiting parameters desired can be substituted into the analysis performed, depending on agency best management practices, management objectives or other factors and allows for customization of the harvest system classification.

Table 3.1 Harvest system scenarios for varying management situations

Scenario 1				
Harvest System	**Variant**	**Operable Slope**	**Forwarding/ Skidding Distance**	**Minimum Merch. Volume**
Buncher/Skidder	A	0 – 35%	< / > 180 m	29 m^3/ha
	B	0 – 45%	< / > 180 m	29 m^3/ha
Excaliner/ Hand Fell	A	> 35%	< 250 m	29 m^3/ha
	B	> 45%	< 250 m	29 m^3/ha
Swing Yarder/ Hand Fell	A	> 35%	> 250 m	29 m^3/ha
	B	> 45%	> 250 m	29 m^3/ha
Scenario 2				
Harvest System	**Variant**	**Operable Slope**	**Forwarding/ Skidding Distance**	**Minimum Merch. Volume**
Buncher/Skidder	A	0 – 35%	> 180 m	29 m^3/ha
	B	0 – 45%	> 180 m	29 m^3/ha
Shovel Harvester	A	0 – 35%	< 180 m	29 m^3/ha
	B	0 – 45%	< 180 m	29 m^3/ha
Excaliner/ Hand Fell	A	> 35%	< 250 m	29 m^3/ha
	B	> 45%	< 250 m	29 m^3/ha
Swing Yarder/ Hand Fell	A	> 35%	> 250 m	29 m^3/ha
	B	> 45%	> 250 m	29 m^3/ha
Scenario 3				
Harvest System	**Variant**	**Operable Slope**	**Forwarding/ Skidding Distance**	**Minimum Merch. Volume**
Buncher/Skidder	A	0 – 35%	> 180 m	29 m^3/ha
	B	0 – 45%	> 180 m	29 m^3/ha
Shovel Harvester	A	0 – 35%	< 180 m	29 m^3/ha
	B	0 – 45%	< 180 m	29 m^3/ha
Tethered Shovel	A	35 – 80%	< 180 m	29 m^3/ha
	B	45 – 80%	< 180 m	29 m^3/ha
Excaliner/ Hand Fell	A	> 35%	< 250 m	29 m^3/ha
	B	> 45%	< 250 m	29 m^3/ha
Swing Yarder/ Hand Fell	A	> 35%	> 250 m	29 m^3/ha
	B	> 45%	> 250 m	29 m^3/ha

For the purposes of this study, it was assumed that all skidding and forwarding for all harvest systems would occur directly parallel to the average azimuth aspect of the stand. Therefore, all skidding and forwarding occurred either directly up or downslope. To facilitate rapid and efficient measurements of all stands, an R script was developed that calculated all max forwarding or skidding distances. All code development was completed in the statistical programming environment R. With the aspect of each stand known, the script performed a sweep perpendicular to the aspect at 50 points along the width of the stand polygon measuring distance. The max forwarding/skidding distance within the polygon shapefile was then determined. With all necessary forest and site metric data available for the harvest system classification for the three scenarios, classification queries were developed and executed in ArcMap. Maps and resulting attributes were collected from the analysis providing both visual and quantifiable results from the harvest system classifications.

Moving through subsequent scenarios within the two variants and introducing new innovative harvest systems is showing areas where these systems may prove effective alternatives, resulting in more efficient operations and lower costs as compared to the traditional systems. The analysis will show where these innovative systems are potential alternatives and if they However, more analysis outside the scope of this project will need to be performed to determine the optimal harvest system per stand.

3.4 Results

The stand level predictions across the 2627 study site stands for trees per hectare, basal area and merchantable volume are shown in Figure 3. These stand level estimates are resultant of the random forest models' predictions derived from the 405 square meter resolution rasters for each of the forest metrics and average slope topographic metric.

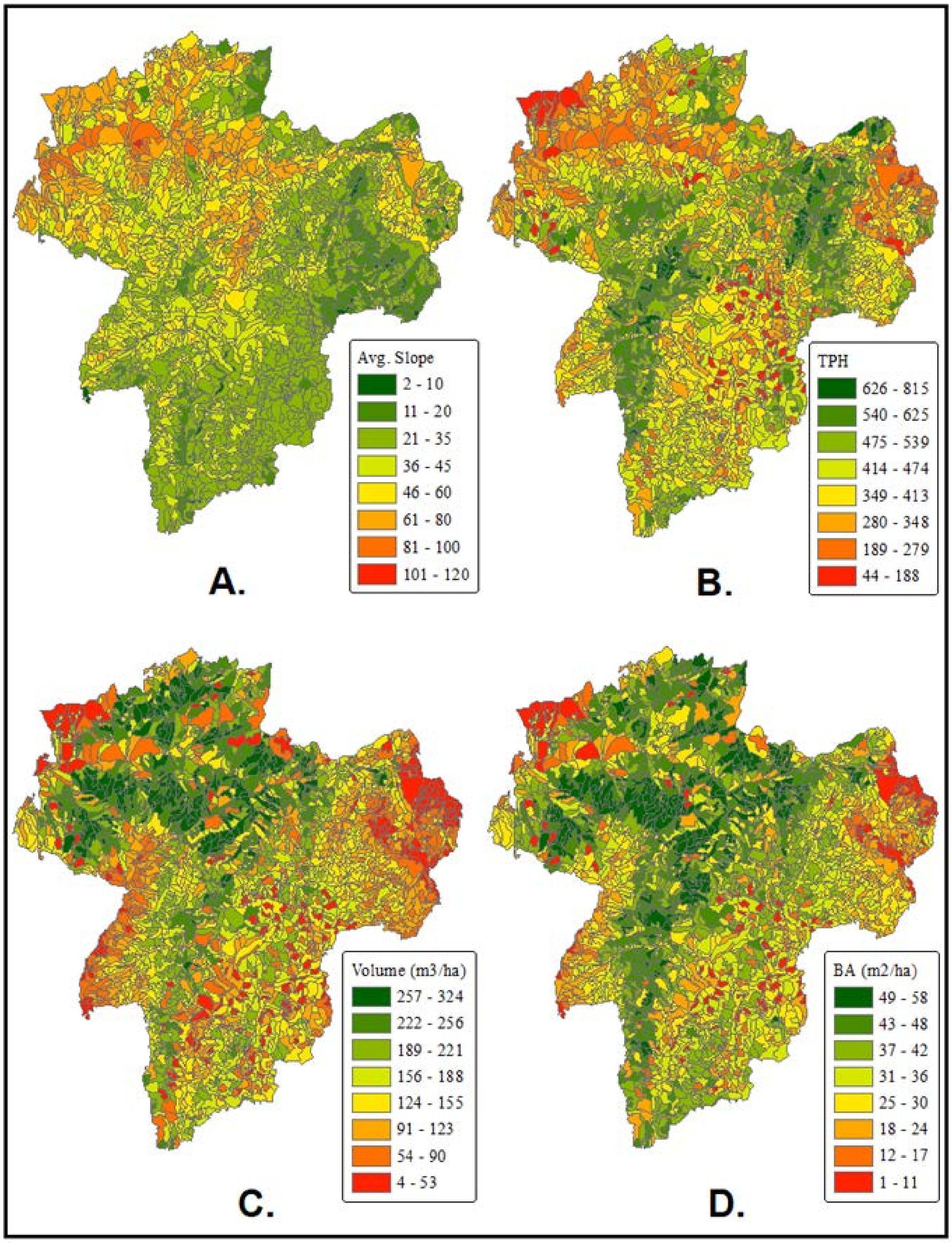

Figure 3.3 Stand-level averages for lidar-derived forest and topographic metrics for Slate Creek study area. Errors (RMSE) associated with map B) are 200.08 trees per hectare, map C) are 78.66 m^3/ha and map C) are 12.71 m^2/ha.

Table 2 shows quality estimates for the random forest models developed for basal area, trees per hectare and merchantable volume in terms of model accuracy, RMSE, mean estimate value and R-squared.

Table 3.2 Random forest model quality assessment

Random Forest	Prediction Mean	RMSE	R-Squared	Accuracy (%)
Trees Per Hectare	405.57 tph	200.08	0.54	70.3
Basal Area	36.57 m^2/ha	12.71	0.65	75.6
Merchantable Volume	180.69 m^3/ha	78.66	0.56	71.9

For all random forest models, the root mean square error was less than 50% of the prediction means for the forest metrics, within the range considered acceptable for our analysis. Additionally, the model accuracies of 70.3%, 75.6% and 71.9% for the trees per hectare, basal area, and merchantable volume forests respectively were captured.

Spatial analysis and querying of the forest and topographic metrics derived from lidar analysis produced maps of the three harvest system scenarios (Figure 4). From the maps, it is clear the introduction of additional harvest systems in Scenario 2 and Scenario 3 results in a recognizable difference in the classification of harvest systems across the 2,627 stand, 30,042 hectare (74,232 acre) study area in both variant situations (Figure 4). Overall, the introduction of the shovel harvester system in Scenario 2 resulted in a change of areas classified as feller-buncher and skidder of 31 percent and 46 percent of the overall area for variant A and B respectively. In the case of both variants, the area lost to the feller-buncher and skidder system was alternatively classified shovel harvester (Table 3).

Between Scenario 2 and Scenario 3, the tethered shovel system was introduced as an alternative to the excaliner and hand fell system resulting in a decrease of area classified as excaliner and hand fell system of 34 and 19 percent of the overall study area for variant A and B respectively (Table 3). A change of classification of 10,260 hectares (25,359 acres) for variant A and 5,830 hectares (14,405 acres) for variant B from excaliner/ hand-fell to tethered shovel was shown.

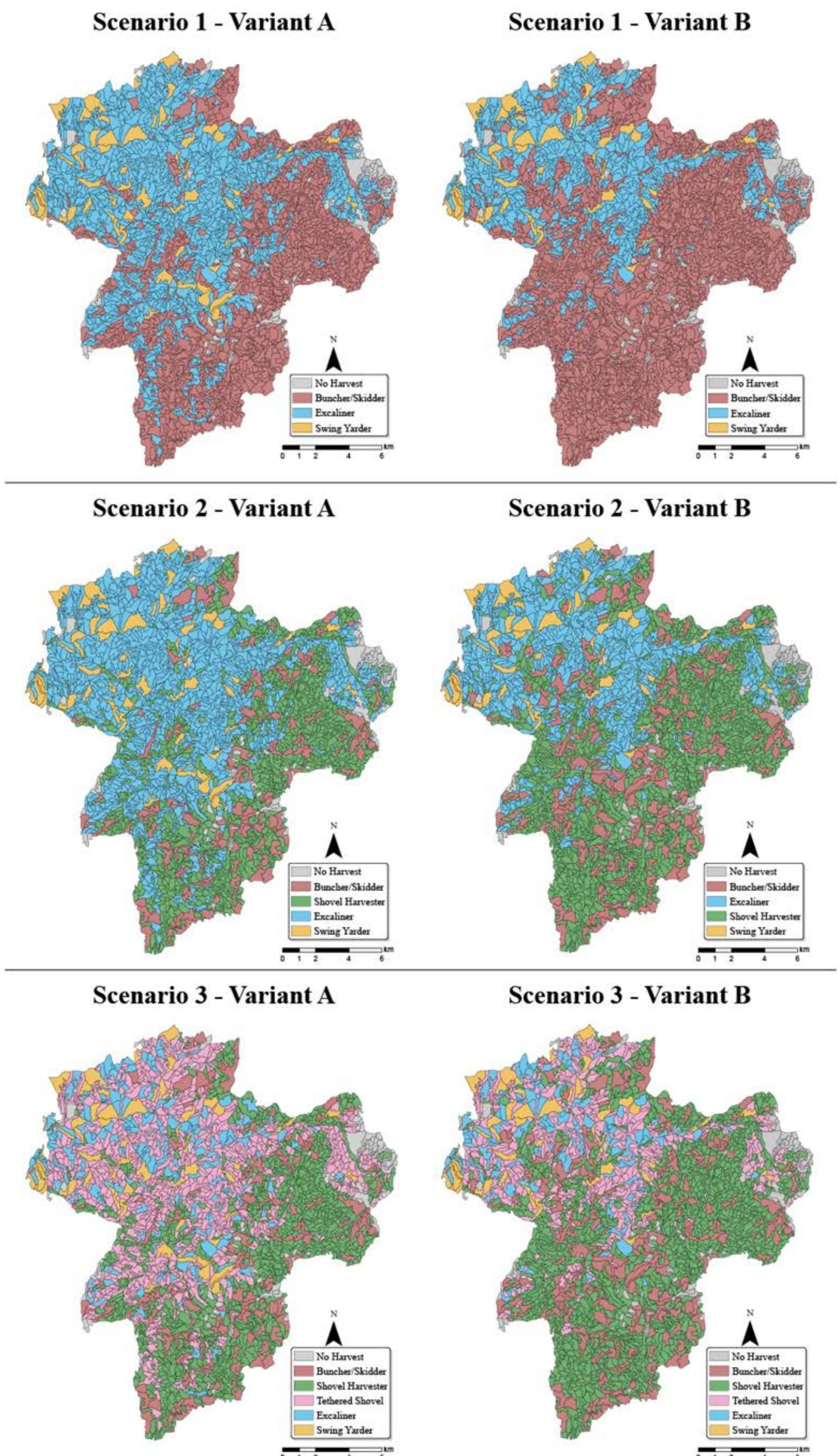

Figure 3.4 Harvest system selection maps for two variations of three harvest scenarios

In all instances, the swing yarder and hand-fell system remained constant for stand and area classification. This is because the swing yarder and hand-fell system represents stands that exceed the maximum forwarding distance for all other harvest systems in this study, resulting in no feasible alternative. Additionally, the number of stands and resultant hectares classified as no harvest remained constant through all scenarios.

Table 3.3 Harvest system classification summary table for two variants of three scenarios

Scenario 1						
Harvest System	Stands		Hectares (Acres)		Area Proportion	
Variant	A	B	A	B	A	B
No Harvest	91	91	1,109 (2,740)	1,109 (2,740)	0.04	0.04
Feller-Buncher/ Skidder	1,201	1,726	12,811 (31,657)	18,940 (46,801)	0.42	0.63
Excaliner/ Hand Fell	1,278	767	14,049 (34,716)	8,422 (20,810)	0.47	0.28
Swing Yarder/ Hand Fell	57	43	2,073 (5,119)	1,571 (3,881)	0.07	0.05
	2,627	2,627	30,042 (74,232)	30,042 (74,232)	1.00	1.00
Scenario 2						
Harvest System	Stands		Hectares (Acres)		Area Proportion	
Variant	A	B	A	B	A	B
No Harvest	91	91	1,109 (2,740)	1,109 (2,740)	0.04	0.04
Feller-Buncher/ Skidder	139	218	3,425 (8,463)	5,222 (12,904)	0.11	0.17
Shovel Harvester	1,062	1,508	9,386 (23,194)	13,718 (33,897)	0.31	0.46
Excaliner/ Hand Fell	1,278	767	14,049 (34,716)	8,422 (20,810)	0.47	0.28
Swing Yarder/ Hand Fell	57	43	2,073 (5,119)	1,571 (3,881)	0.07	0.05
	2,627	2,627	30,042 (74,232)	30,042 (74,232)	1.00	1.00
Scenario 3						
Harvest System	Stands		Hectares (Acres)		Area Proportion	
Variant	A	B	A	B	A	B
No Harvest	91	91	1,109 (2,740)	1,109 (2,740)	0.04	0.04
Feller-Buncher/ Skidder	139	218	3,425 (8,463)	5,222 (12,904)	0.11	0.17
Shovel Harvester	1,062	1,508	9,386 (23,194)	13,718 (33,897)	0.31	0.46
Tethered Shovel	1,064	618	10,262 (25,359)	5,830 (14,405)	0.34	0.19
Excaliner/ Hand Fell	214	149	3,787 (9,357)	2,592 (6,405)	0.13	0.09
Swing Yarder/ Hand Fell	57	43	2,073 (5,119)	1,571 (3,881)	0.07	0.05
	2,627	2,627	30,042 (74,232)	30,042 (74,232)	1.00	1.00

It was found that adding 10 percent slope to the operable slope limit in variant B resulted in an increase of land classified as ground-based logging systems (feller-buncher/ skidder) of

6,132 hectares (15,144 acres) or 21 percent for Scenario 1. In Scenario 2, there were 4,334 hectares (10,703 acres) more classified as shovel harvester in variant B than A. In Scenario 3, there were 4,430 hectares (10,954 acres) more classified as tethered shovel in variant A than in variant B due to the higher area initially characterized as steep slope, cable ground.

Variant A resulted in an initial ground-based harvest system classification of 42 percent of the overall study area, with 54 percent classified as cable harvest and the remaining 4 percent defined as no harvest. These percentages remained consistent through all 3 scenarios when comparing ground based and cable or cable assisted systems. In variant B harvest system classification, the additional 10 percent slope added to the upper bounds of the operable slope of the ground-based systems resulted in an overall ground-based system classification of 63 percent and 33 percent cable system classification.

3.5 Discussion

Our method of using LiDAR to characterize operational stand characteristics to pre-plan forest operations and comparative analysis of alternative harvest options prior to field layout and implementation proved effective. The random forest models developed to predict forest metrics across the study area returned accuracies exceeding 70% which was deemed acceptable for the subsequent analysis performed using the model predictions. In variant A of the harvest system classification analysis, we found that the ground-based shovel logging was a feasible alternative to the feller-buncher system in 1,062 stands. Comparatively, ground-based shovel logging systems provided a significant alternative to the feller-buncher and grapple skidder in variant B on 1508 individual stands. Similarly, the tethered shovel harvester system was found to be a significant alternative to the excaliner in 1,064 stands for variant A and 618 stands for variant B. From an operational standpoint, the potential implementation of the shovel harvester in lieu of the feller-buncher and grapple skidder system means that one machine could be used to harvest these stands rather than two. This may lead to lower fuel, labor and maintenance costs, resulting in lower total logging costs. The ability to match an appropriate harvest system with operability constraints of forest and topographic conditions is the first step in increasing productivity and reducing costs. However, stand-level logging costs for the two systems should be estimated and compared prior to decision-making about preferred options. The high production and cost effectiveness of shovel logging increases its feasibility, even in mountainous terrain (Fisher 1999). Site impacts caused by shovel logging are inherently less than other ground based systems, making shovel logging a favorable alternative for sensitive sites (Fisher 1999). Self-leveling capabilities of new shovels increase the safe, effective operating capabilities of the machines, making the use of shovel logging more feasible across a wider range of sites, especially in the Inland Northwest.

Increasing the slopes on which ground-based harvest machinery are allowed to operate, especially within the National Forest system, is an important consideration when attempting to maximize operational production and safety. Increasing the upper bounds of the operable slope for the ground-based systems by 10 percent slope resulted in an increase in overall operable ground of 21 percent of our study area. This equated to over 6,300 ha. Increased safety associated with mechanized felling using tethered and untethered shovel harvesters is an important benefit when considering increasing the allowable slopes of ground-based systems. This is especially relevant in the context of the Slate Creek study area, where beetle killed stands present hazardous working conditions for ground workers. Classifying feasible stands to incorporate these alternative harvest systems means fewer workers outside the protection of enclosed machine cabs. Logging costs for ground based shovel logging have been found to be

40% less than some cable alternatives as well, further supporting their implementation (Fisher 1999).

The ground-based shovel harvester systems, both tethered and untethered, are gaining traction as popular harvest methods in the inland northwest. Delineating areas where harvest systems can be incorporated into management practices may in turn promote effective forest management by creating safer working conditions, and increasing harvest production. This is done by providing the tools necessary for decisions to be made that result in the incorporation of the most effective and appropriate management strategies considering forest and topographic features as well as innovative technologies and processes.

Accuracy with which forest and topographic metrics can be derived and predicted from lidar data for use in resource management is increasing (Reutebuch et al. 2005). The development of automated algorithms for detecting and delineating individual tree crowns has made the application of this data in precision forestry applications more feasible (Zhen et al. 2016). Research delineating individual tree locations and individual tree volume estimation continues to advance our understanding and utilization of remotely sensed lidar data and provide opportunities to advance precision forestry in new ways (Falkowski et al. 2006; Chen et al. 2007; Akay et al. 2009; Gupta et al. 2013; Zhen et al. 2016; Barnes et al. 2017). Methods to develop these predictions, however, still need to be developed and current applications are limited. At this point in time, lidar provides a valuable data resource for predictions and depictions of forest and topographic characteristics useful for stand- and landscape scale harvest system classification, as shown in this study.

It is understood that when applying this methodology for harvest system classification in additional areas that the large number of plots used to train and test the random forest models for forest metrics may not be available. To address this concern, random forest models were developed for trees per hectare, basal area and merchantable volume following the same methodology previously used, but exploring the affect that sample size had on model accuracy and strength. Random forest models were developed using varying sample plots, from 10 up to 91 plots. The results from the additional random forest model quality assessments are shown in Figures 3.5 for the trees per hectare random forests model, 3.6 for the merchantable volume random forests model, 3.7 for the basal area random forests model and as summary tables assessing model accuracies for all three forest metrics in Appendix A.

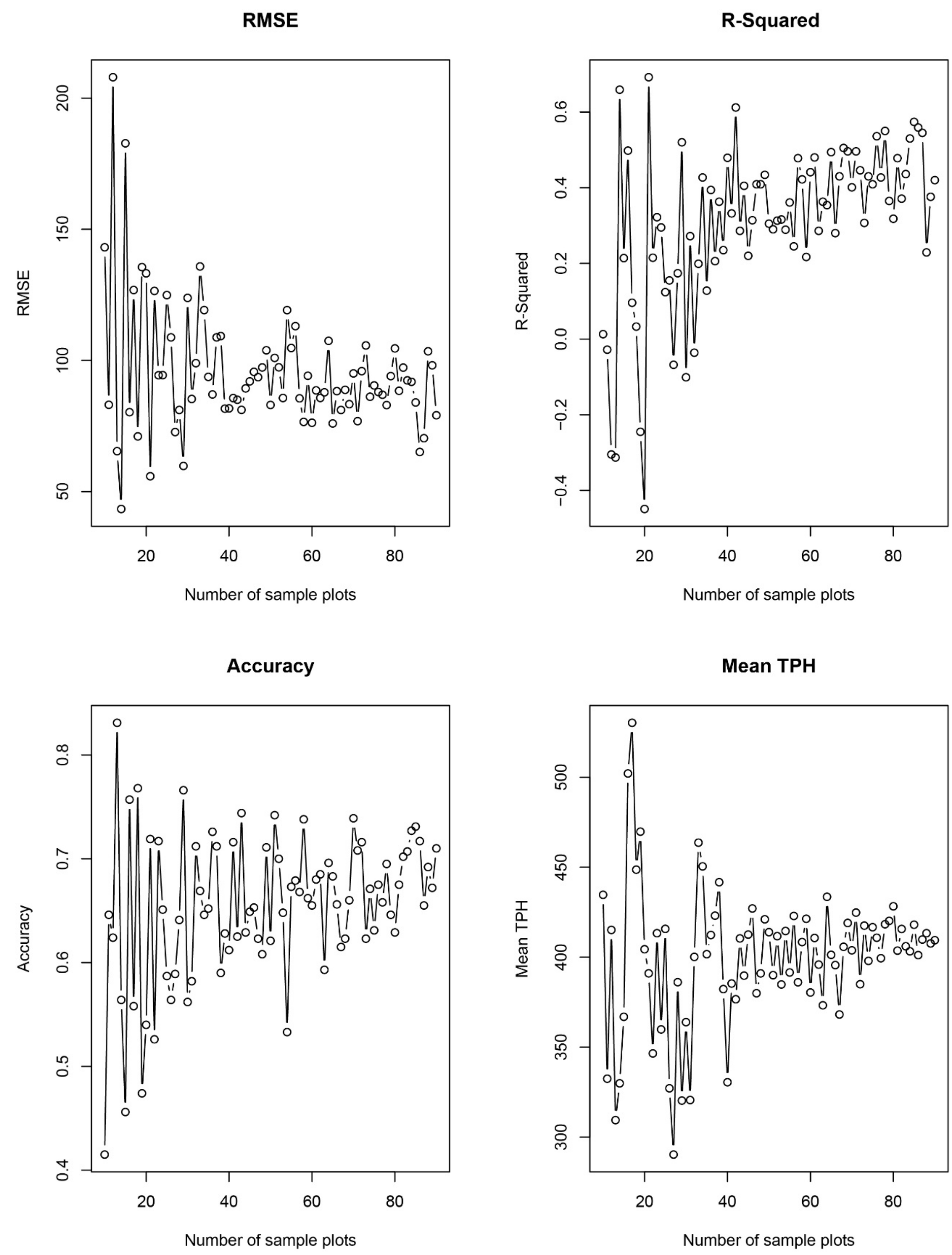

Figure 3.5 Root mean squared error, R-squared, Accuracy and Prediction Mean plots for Trees per Hectares representing sample plots of 10 up to 90

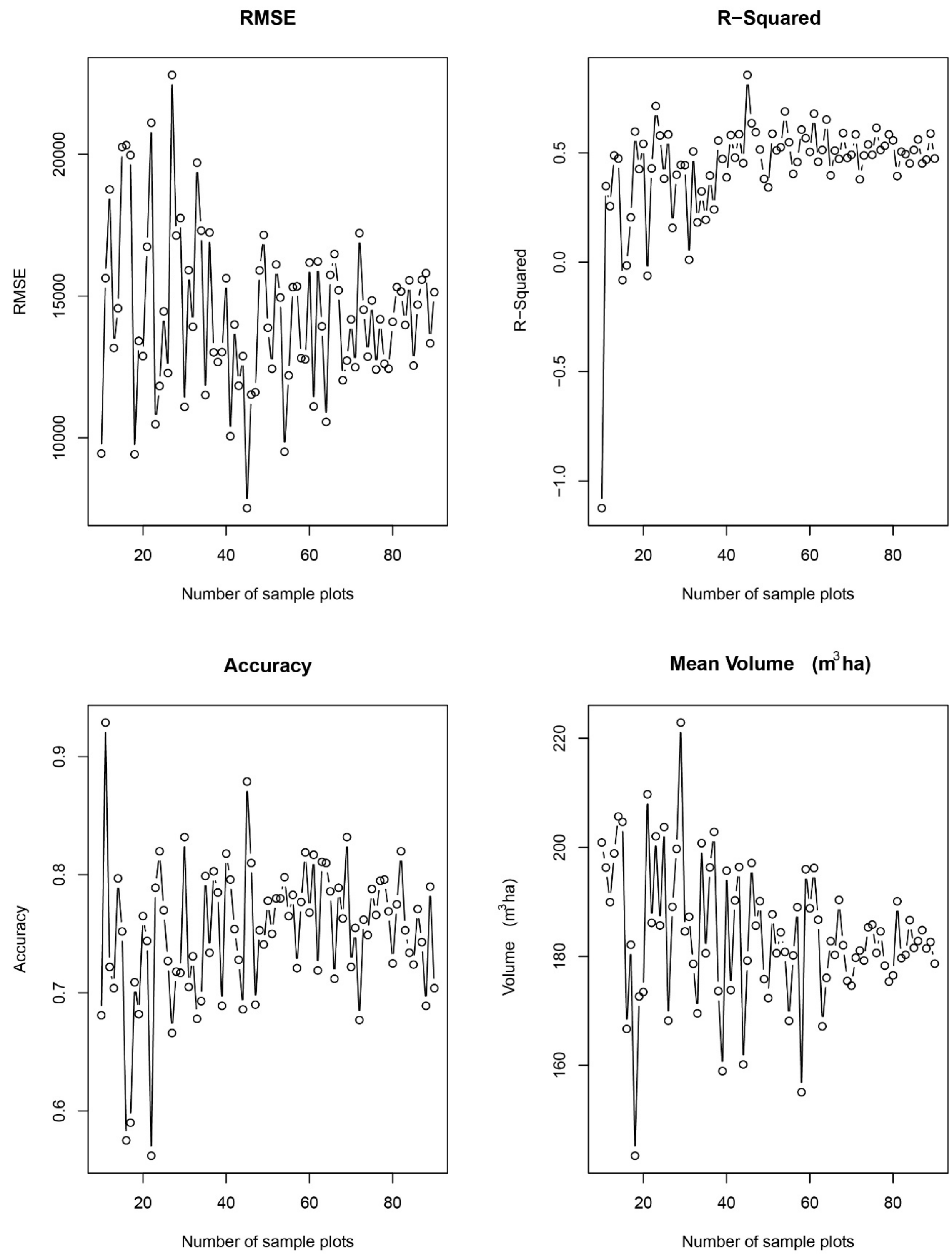

Figure 3.6 Root mean squared error, R-squared, Accuracy and Prediction Mean plots for Merchantable Volume representing sample plots of 10 up to 90

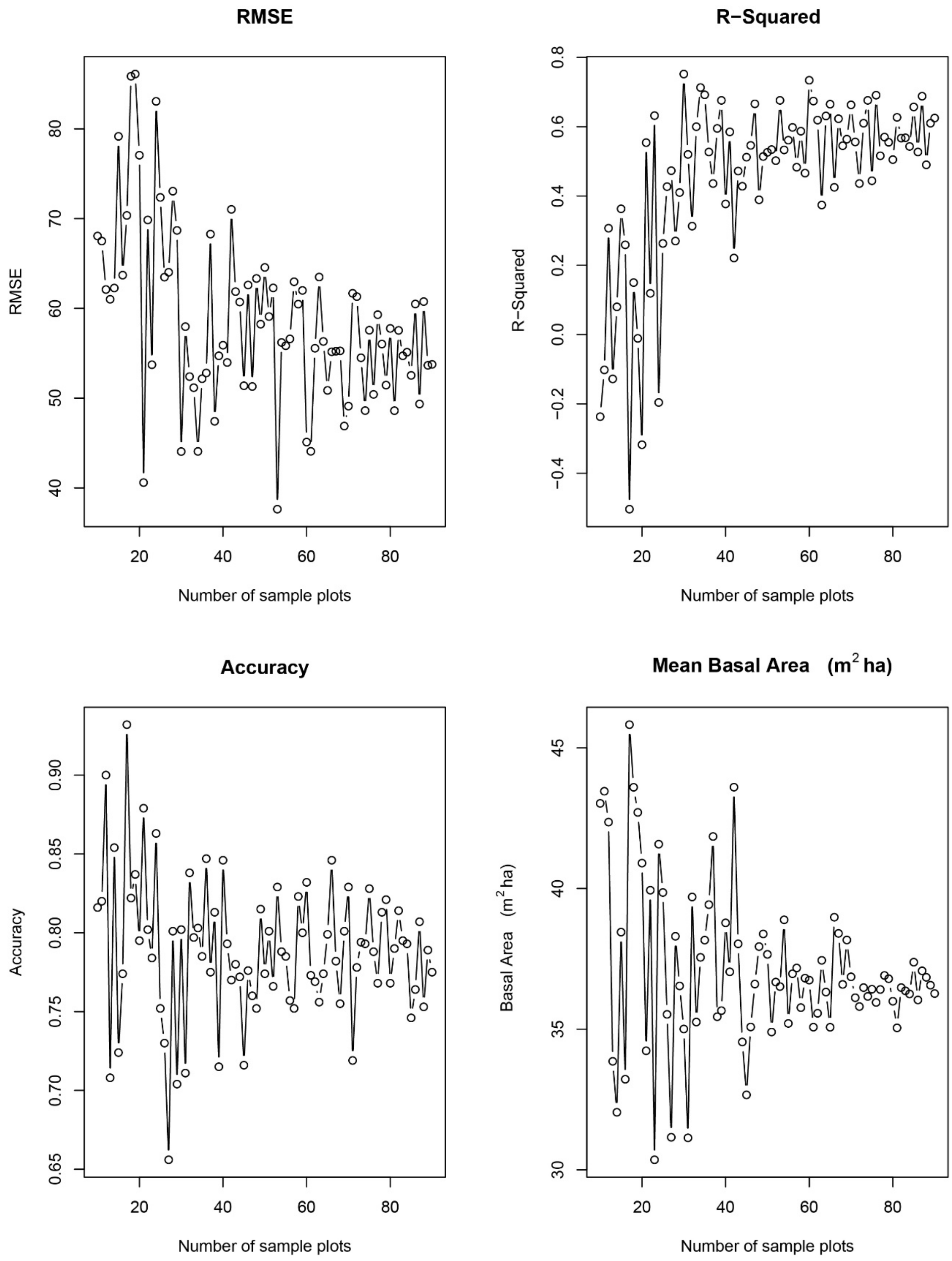

Figure 3.7 Root mean squared error, R-squared, Accuracy and Prediction Mean plots for Basal Area representing sample plots of 10 up to 90

From the figures, it is evident that for all three models, the RMSE decreases and the R-squared values increase which is indicative of an improving model. In several instances where the R-squared value is a negative value represents very poor models. These cases were only found to exist in small sample sizes. As the number of sample plots increased, the variation between the prediction means for all forest metrics between subsequent plots became more consistent. With a larger number of sample plots, the overall variability of the study area was better represented and random samples of predominantly high or low values were less likely to skew the data. Accuracies of the models stayed relatively consistent for all sample sizes, though less variability was found between subsequent numbers of sample plots once the sample sizes increased. This indicates that larger sample sizes produce more consistent random forests models for forest metric predictions. For all accuracy assessment values for all three forest metrics, it appears that values became more consistent and improved when the sample plot number exceeded approximately 40 plots. Therefore, it can be assumed that comparable random forests models and resulting prediction accuracies can be achieved with access to fewer training and testing plots. However, accuracies of predictions may be adversely impacted once the number of sample plots drops below a threshold. It is unclear from our analysis what factors may affect this threshold.

Efficiently performing harvest system classifications at the landscape scale using lidar-derived metrics will lead to continuing work further utilizing these data in an operational context (Figure 5). Combining these classifications with stand-level logging cost estimates in future work provides the basis for determining the optimal harvest system at the stand-level in subsequent analysis. Additionally, stand-level production and logging cost estimates will provide the foundation for performing estate-level harvest scheduling analysis with stand-specific logging cost estimates, rather than assumed values.

Lidar-derived harvest system classifications can also be integrated with individual tree-level harvest simulation and real-time decision support, further building on the foundational work developed in this study. Keefe et al. (2014) outlined the use of GNSS-RF (geographic navigation satellite system with radio frequency) as a method to support real-time analysis and model-based decision support in forest operations. Becker et al. (2017), Grayson et al. (2016) and Zimbelman et al. (2017) all explored the application of GNSS-RF technologies in operational forestry and logging safety applications. The use of lidar-derived forest and topographic metrics for harvest system selection described in this study will further advance this work and other facets of forest operations.

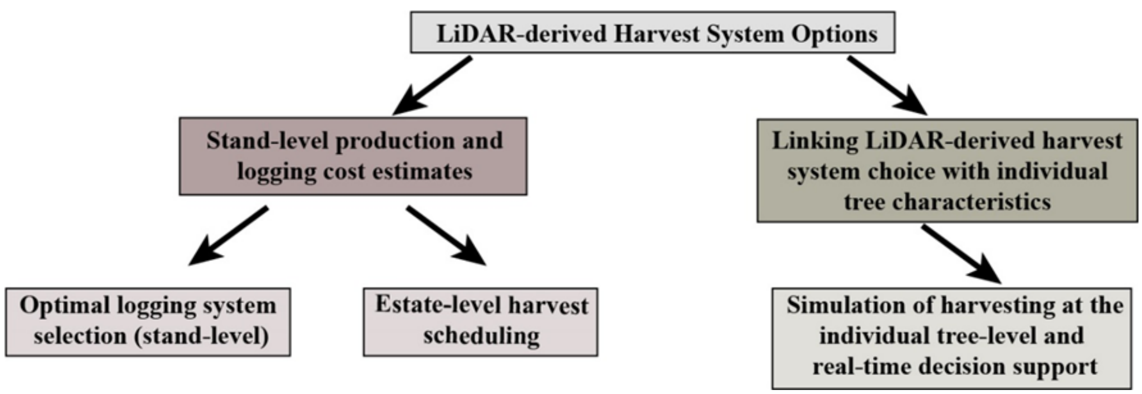

Figure 3.8 Future work addressing operational applications from LiDAR-derived harvest system classifications

As technologies and equipment continue to advance in the future, operations foresters and forest planners can increasingly utilize and incorporate lidar analysis into current practices to increase harvest production, minimize costs, and encourage long-term sustainable forest management practices. Our results showed the significant potential for characterizing the appropriateness of new and logging systems at the stand and landscape scale, and should be further explored in future studies.

3.6 References

Abbas D, Fulvio FD, Spinelli R. 2017. European and United States perspectives on forest operations in environmentally sensitive areas. Scan J For Res. 1-14.

Acosta M, Corral S. 2017. Multicriteria decision analysis and participatory decision support systems in forest management. Forests. 8(116):1-15.

Acuna M, Skinnell J, Evanson T, Mitchell R. 2011. Bunching with a Self-levelling Feller-Buncher on Steep Terrain for Efficient Yarder Extraction. Croat J For Eng. 32(2):521–531.

Adams JD, Visser RJM, Prisley SP. 2003. Modelling steep terrain harvesting risk using GIS. Proceedings of Austro2003: High Tech Forest Operations for Mountainous Terrain; October 5-9; Schlaegl, Austria.

Akay AE, Karas IR, Sessions J, Gundogan R. 2004. Using high-resolution digital elevation model for computer-aided forest road design. Proceedings of the International Society of Photogrammetry and Remote Sensing Congress; July; Istanbul, Turkey.

Akay AE, Oguz H, Karas IR, Aruga K. 2009. Using LiDAR technology in forestry activities. Environ Monit Assess. 151:117-125.

Akay AE, Sessions J. 2005. Applying the decision support system, TRACER, to forest road design. W J App For. 20(3):184-191.

Alam M, Acuna M, Brown M. 2013. Self-leveling feller-buncher productivity based on lidar-derived slope. Croat J For Eng. 34(2):273-281.

Amishev D, Evanson T. 2010. Innovative methods for steep terrain harvesting. Proceedings of FORMEC Forest Engineering: Meeting the Needs of Society and the Environment; July 11-14; Padova, Italy.

Amishev D. 2017. International research on winch-assist equipment. Proceedings of the Western Region Council of Forest Engineering (WR COFE): Improving Forest Harvest Operations; January 19; Eugene, OR.

Andersson B, Young G. 1998. Harvesting coastal second-growth forests: Summary of harvesting system performance. Pointe-Claire(QC): Forest Engineering Research Institute of Canada. Report No.:TR-120.

Aruga K, Sessions J, Akay AE. 2005. Application of an airborne laser scanner to forest road design with accurate earthwork volumes. J For Res. 10:113-123.

Barkley Y, Brooks R, Keefe R, Kimsey M, McFarland A, Schnepf Chris. 2015. Idaho Forestry Best Management Practices Field Guide. Moscow: University of Idaho.

Barger M, Messerlie E, Rheinberger S. 2015. Skyline XL 15.1 - Skyline profile and payload analysis. Downloaded on April 15, 2016 from: USFS PNW Forest Products Programs and Software. USDA FS PNW Research Station: Portland, OR.

Barnes C, Balzter H, Barrett K, Eddy J, Milner S. 2017. Individual tree crown delineation from airborne laser scanning for diseased larch forest stands. Remote Sensing. 9(231):1-20.

Becker RM, Keefe RF, Anderson NM. 2017. Use of real-time GNSS-RF data to characterize the swing movements of forestry equipment. Forests. 8(2):44.

Bell CK, Keefe RF, Fried JS. 2017. Validation of the OpCost logging cost model using contractor surveys. Int J For Eng. 28(2):73-84.

Bell CK, Keefe RF. 2014. FVS-OpCost: a new forest operations cost simulator linked with FVS. Proceedings of the Council on Forest Engineering (COFE): Global Harvest Technology; June 22-25; Moline, IL.

Breiman L. 2001. Random forests. Mach. Learn. 45(1): 5–32.

Brinker RW, Kinard J, Rummer R, Lanford B. 2002. Machine rates for selected forest harvesting machines. Auburn (AL) Alabama Agricultural Experiment Station, Auburn University; 32 p.

Cavalli R. 2015. Forest operations in steep terrain. Proceedings of the Conference CROJFE 2015 Forest Engineering: Current Situation and Future Challenges; March 18-20; Zagreb, Croatia.

Chen Q, Gong P, Baldocchi D, Tian YQ. 2007. Estimating basal area and stem volume for individual trees from lidar data. Photogrammetric Eng Remote Sensing. 73(12):1355-1365.

Chung W, Sessions J, Heinimann HR. 2004. An application of a heuristic network algorithm to cable logging layout design. Int J For Eng. 15(1):11-24.

Davis, C., & Reisinger, T. 1990. Evaluating terrain for harvesting equipment selection. J For Eng. 2(1):9–16.

Eliasson L. 1999. Simulation of thinning with a single-grip harvester. For Sci. 45(1):26-34.

Evans JS, Murphy MA. 2017. rfUtilities: Random forests model selection and performance evaluation. R package version 2.0-1, https://cran.r-project.org/web/packages/rfUtilities/index.html.

Falkowski MJ, Smith AMS, Hudak AT, Gessler PE, Vierling LA, Crookston NL. 2006. Automated estimation of individual conifer tree height and crown diameter via two-dimensional spatial wavelet analysis of lidar data. Can J Remote Sensing. 32(2):153-161.

Fisher J. 1999. Shovel logging: cost effective systems gains ground. Proceedings of International Mountain Logging and 10th Pacific Northwest Skyline Symposium; March 28-April 1; Corvallis, OR. p.61-67.

Gan Z, Zhong L, Li Y, Guan H. 2015. A random forest based method for urban object classification using LiDAR data and aerial imagery. Proceedings of the 23rd International Conference on Geoinformatics; June 19-21; Wuhan, China.

Gellerstedt S. 1998. A self-levelling and swivelling forestry machine cab. J For Eng. 9(1):7-16.

Grayson LM, Keefe RF, Tinkham WT, Eitel JUH, Saralecos JD, Smith AMS, Zimbelman EG. 2016. Accuracy of WAAS-enabled GPS-RF warning signals when crossing a terrestrial geofence. Sensors. 16(6):912.

Greulich FR, Hanley DP, McNeel JF, Baumgarter D. 2001. A primer for timber harvesting. Boise (ID): USDA- Natural Resource Conservation Service. Report No.: EB1316.

Gupta S, Weinacker H, Sterenczak K, Koch B. 2013. Single tree delineation using airborne lidar data. Euro Scientific J. 9(32):405-435.

Hartsough BR, Zhang X, Fight RD. 2001. Harvesting cost model for small trees in natural stands in the interior northwest. For Prod J. 51(4):54-61.

Heinimann HR. 1998. A computer model to differentiate skidder and cable-yarder based road network concepts on steep slopes. J For Res. 3:1-9.

Hudak AT, Bright BC, Pokswinski SM, Loudermilk EL, O'Brian JJ, Hornsby BS, Klauberg C, Silva CA. 2016. Mapping forest structure and composition from low-density LiDAR for informed forest, fuel, and fire management at Englin Air Force Base, Florida, USA. Can J Remote Sensing. 42:411-427.

Johnson LR, Page-Dumroese D, Han HS. 2005. Effects of machine traffic on the physical properties of ash-cap soils. In: Page-Dumroese D, Miller R, Mital J, McDaniel P, Miller D, tech. eds. 2007. Proceedings of the RMRS-P-44: Volcanic-Ash-¬Derived Forest Soils of the Inland Northwest: Properties and Implications for Management and Restoration; November 9-10; Coeur d'Alene, ID. Fort Collins, CO: U.S. Department of Agriculture, Forest Service, Rocky Mountain Research Station.

Keefe R, Anderson N, Hogland J, Muhlenfeld K. 2014. Woody biomass logistics. In: Karlen DL, editor. Cellulosic energy cropping systems. Hoboken (NJ): John Wiley & Sons. p. 251–278.

Keefe RF. 2014. Applications of multi transmitter GPS-VHF in forest engineering. Proceedings of the 47th International Symposium on Forestry Mechanization and 5th International Forest Engineering Conference; September; Gerardmer, France.

Kühmaier M, Stampfer K. 2010. Development of a multi-attribute spatial decision support system in selecting timber harvesting systems. Croatian J For Eng. 31:75–88.

Lan Z. 2001. A Cost Model for Machine Operation in Wood Cutting and Extraction, ECOWOOD – Activities at the University of Helsinki Partner Number 4, 2001-03-22, QLK5-CT-1999-00991, Finland.

Largo S, Han HS, Johnson L. 2004. Productivity and cost evaluation for non-guyline yarders in Northern Idaho. Proceedings of the Council on Forest Engineering (COFE): Machines and People, The Interface; April 27–30; Hot Springs, AK.

Laukkanen S, Palander T, Kangas J, Kangas A. 2005. Evaluation of the multicriteria approval method for timber-harvesting group decision support. Silva Fenn. 39(2):249–264.

Liaw A, Wiener M. 2002. Classification and Regression by randomForest. R News 2(3), 18--22. https://cran.r-project.org/web/packages/randomForest/index.html.

MacDonald AJ. 1999. Harvesting systems and equipment in British Columbia, FERIC Handbook. ISSN 0707-8355. No. HB-12. p.197.

Matthews DM. 1942. Cost control in the logging industry. McGraw-Hill. New York, New York and London, UK. 374 p.

McKenzie DW, Richardson BY. 1978. Feasibility study of self-contained tethered cable system for operational equipment on slopes of 20 to 75%. J Terramechanics. 15(3):113-127.

Moye FJ, Hackett WR, Blakley JD, Snider LG. 1988. Regional geologic setting and volcanic stratigraphy of the Challis volcanic field, central Idaho. In: Link PK, Hackett WR, editors. Guidebook to the geology of central and southern Idaho. Idaho Geological Survey Bulletin; p.87-97.

Page-Dumroese DS. 1993. Susceptibility of volcanic ash-influenced soil in northern Idaho to mechanical compaction. Forest Service, Intermountain Research Station. Research Note: INT-409.

R: A language and environment for statistical computing. 2016. Vienna(Austria): R Foundation for Statistical Computing R Core Team; [accessed 2016 September 10]. https://www.R-project.org/.

Reisinger T, Davis C. 1986. A map-based decision support system for evaluating terrain and planning timber harvests. American Society of Agricultural Engineers. 29(5):1199–1203.

Reutebuch SE, Andersen H, McGaughey RJ. 2005. Light detection and ranging (LIDAR): An emerging tool for multiple resource inventory. J For. 286-292.

Rodriguez-Galiano VF, Ghimire B, Rogan J, Chica-Olma M, Rigol-Sanchez JP. 2012. An assessment of the effectiveness of random forest classifier for land-cover classification. ISPRS J Photogrammetry and Remote Sensing. 67(2012):93-104.

Sessions J, Leshchinsky B, Chung W, Boston K, Wimer J. 2017. Theoretical stability and traction of steep slope tethered feller-bunchers. For Sci. 63(2):192-200.

Stampfer K, Lexer MJ, Vacik H, Hochbichler E, Durrstein H, Spork J. 2001. Cones – A computer based multiple criteria decision support tool for timber harvest planning in steep terrain. Proceedings of the Council on Forest Engineering (COFE): Appalachian Hardwoods: Managing Change; July 15-18; Snowshoe, WV.

Strandgard M, Alam M, Mitchell, R. 2014. Impact of slope on productivity of a self-levelling processor. Croat J For Eng. 35(2):193–200.

Suvinen A. 2006. A GIS-based simulation model for terrain tractability. J of Terramechanics, 43(4):427–449.

Talbot B, Nordfjell T, Suadicani K. 2003. Assessing the utility of two integrated harvester-forwarder machine concepts through stand-level simulation. Int J For Eng. 14(2), 31-34.

Visser R, Stampfer K. 2015. Expanding ground-based harvesting onto steep terrain: A review. Croat J For Eng. 36(2):321-331.

Wang J, Greene WD, Stokes BJ. 1998. Stand, harvest, and equipment interactions in simulated harvesting prescriptions. For Products J. 48(9):81-86.

Wang J, LeDoux CB. 2003. Estimating and validating ground-based timber harvesting production through computer simulation. For Sci. 49(1):64-76.

Zhen Z, Quakenbush LJ, Zhang L. 2016. Trends in automatic individual tree crown detection and delineation- Evolution of LiDAR data. Remote Sensing. 8:1-26.

Zimbelman EG, Keefe RF, Strand EK, Kolden CA and Wempe AM. 2017. Hazards in motion: development of mobile geofences for use in logging safety. Sensors, 17(4):822.

Chapter 4: Thesis Conclusions

As technology continues to advance in the coming years, it is likely that we will continue to see increased application in natural resource management and precision forestry contexts. The ability to define work in forestry using spatially explicit data and corresponding data gathered from additional sensors in becoming increasingly possible as research into and development into innovative applications increases. We successfully defined and characterized the work elements of a shovel using exclusively GNSS-RF recorded data at 90% plus success rates. Using consumer grade GNSS-RF transponders, we accurately determined not only what work task the machine was performing, but also the location of various machine components in space at given times. These promising results set the foundation of future studies further exploring similar methods to define work and production of forestry machines using not only GNSS-RF transponders but additional sensors as well.

Developing a library of activity profiles for forestry machinery and personnel tasks will change the way in which we determine production and interactions of machinery and personnel in the forests. Sharing of these data in real-time provides greater insight into interactions between machinery and ways in which production can be increased while potentially decreasing subsequent costs. Additionally, increasing the connectivity and data sharing capabilities in the forest will increase the situational awareness of all components of an operation. In time, this may lead to increased safety on logging operations and insight into ways to maximize tactical harvest planning.

As access to affordable, user friendly technologies and methods to collect and analyze these data continue to develop, their application in forestry and land management practices is likely to increase. Precision forestry; planning and conducting management on a microsite, stand level; will likely increase as greater insight into operations gathered from GNSS-RF and real-time technologies becomes more available. This will be encouraged further by access to high resolution, remotely sensed data and the derivation and application of spatial data products into management planning.

Using lidar derivation and analysis techniques, we were able to predict forest metrics for trees per hectare, cubic meters per hectare volume, and basal area for our 34,000 hectare Slate Creek study area. Our prediction models returned metrics predictions of at least 70% in all cases which were then used to develop the stand level harvest system selection model. The combination of our lidar derived forest and topographic metrics provided a rich data set which was used in the selection process to determine if innovative, alternative harvest systems were feasible options over traditional harvest systems. In the case of both the shovel harvester and the tethered shovel harvester, we determined that they were feasible alternatives to feller buncher/ grapple skidder systems and excaliner/ hand fell systems respectively across a significant proportion of the area originally classified as the traditional system.

The next step in further refining this model will be to develop production and cost components of the model to predict logging cost estimates for each harvest system across their feasible stands. Doing so will develop a decision support model which shows the optimal system at the stand level based on forest and topographic metrics as well as logging costs. This stand level analysis refined from high resolution data can further be strengthened by coupling it with real-time GNSS-RF data to paint an increasingly detailed picture as to how machinery work across not only the landscape, but within the stand.

Understanding of how forest and topographic metrics affect machine productivity and interactions can be addressed as well. The availability of high resolution spatial data and the collection of subsequent data regarding machine activities in real-time will change the way in which we plan and execute forestry tasks in the future.

This detailed understanding of production and the factors affecting it will provide valuable information to contractors and harvest planners regarding the processes and harvest systems necessary to maximize production and minimize costs across the landscape. This is especially relevant when developing management strategies for beetle-killed and other salvage harvest operations where degraded timber value decreases the feasibility of harvests due to low value. Selecting the optimal harvest system based on forest and topographic metrics will help to reduce overall costs and ensure these necessary harvests are able to be completed across the landscape for future forest health and severe fire threat reduction.

The studies described in this thesis provide foundational methods and results for future work to be built from. As follow-up research occurs and methods and end products are refined, the goal is to develop a library of production models that can be used by operations foresters and contractors to predict logging costs and define work across management areas. Combined with high resolution spatial products and lidar-derived forest metrics, stand level tactical planning for harvests and other management tasks is becoming more of a reality. What many once left the woods to escape is becoming a familiar resource, as technology integration into natural resource management and forest operations continually expands. In time, the way in which data is shared, production is determined, and the scale at which harvest planning and operations are addressed will be starkly different than what was even though possible by previous generations. A clear understanding of not only the capabilities that real-time positional data and remotely sensed possess, but ways to effectively incorporate these into real world management scenarios is integral to capturing the potential benefits these data sources provide for decision support and management execution in forest operations and natural resource management. Precision forestry has long been a novel concept with little application and execution in forest management. However, the methods and products developed in the previous two chapters combine an understanding of real-time and remotely sensed data capabilities to address management challenges and actualize the concept of precision forestry.

Appendix A: Random Forests Extended Sample Tables

Trees per Hectare				
# of Plots	Prediction Mean (TPH)	RMSE	R-Squared	Accuracy (%)
10	434.66	143.12	0.01	41.5
13	309.45	65.40	-0.31	83.1
16	502.09	80.26	0.50	75.7
19	469.76	135.57	-0.25	47.4
22	346.51	126.49	0.22	52.6
25	415.73	124.90	0.12	58.7
28	386.10	81.11	0.17	64.1
31	320.60	85.30	0.27	58.2
34	450.46	119.18	0.43	64.6
37	423.08	108.79	0.21	71.2
40	330.50	81.71	0.48	61.2
43	410.42	81.14	0.29	74.4
46	427.06	95.65	0.31	65.3
49	421.04	103.86	0.43	71.1
52	411.67	97.37	0.31	70.0
55	391.50	104.74	0.36	67.3
58	408.40	76.56	0.42	73.8
61	410.68	88.57	0.48	68.0
64	433.55	107.46	0.35	69.6
67	368.15	81.10	0.43	61.5
70	403.80	95.04	0.40	73.9
73	417.54	105.70	0.31	62.3
76	410.81	87.97	0.54	67.5
79	420.17	94.02	0.37	64.6
82	415.68	97.26	0.37	70.2
85	418.04	83.96	0.57	73.1
88	413.31	103.47	0.23	69.2

Merchantable Volume				
# of Plots	Prediction Mean (m^3/ha)	RMSE	R-Squared	Accuracy (%)
10	200.88	9445.09	-1.12	68.1
13	198.89	13172.34	0.49	70.4
16	166.69	20320.02	-0.02	57.5
19	172.65	13417.14	0.43	68.2
22	186.14	21107.85	0.43	56.2
25	203.73	14459.57	0.38	77.0
28	199.73	17134.96	0.40	71.8
31	187.25	15913.17	0.01	70.5
34	200.77	17305.82	0.32	69.3
37	202.84	13015.36	0.24	80.3
40	195.71	15628.44	0.39	81.8
43	196.40	11838.27	0.59	72.8
46	197.12	11526.40	0.64	81.0
49	175.84	17156.31	0.38	74.1
52	180.60	16113.71	0.51	78.0
55	168.16	12201.89	0.55	76.5
58	155.08	12810.11	0.61	77.7
61	196.22	11106.97	0.68	81.7
64	176.07	10561.98	0.65	81.0
67	190.35	15200.83	0.47	78.9
70	174.64	14179.61	0.49	72.2
73	179.24	14521.21	0.49	76.2
76	180.64	12411.02	0.61	76.6
79	175.37	12437.44	0.58	76.9
82	179.69	15161.06	0.51	82.0
85	181.57	12547.38	0.51	72.4
88	181.46	15808.01	0.47	68.9

Basal Area				
# of Plots	Prediction Mean (m^2/ha)	RMSE	R-Squared	Accuracy (%)
10	43.03	68.06	-0.24	81.6
13	33.86	61.01	-0.13	70.8
16	33.22	63.70	0.26	77.4
19	42.71	86.10	-0.01	83.7
22	39.94	69.85	0.12	80.2
25	39.86	72.36	0.26	75.2
28	38.30	73.05	0.27	80.1
31	31.14	57.97	0.52	71.1
34	37.55	44.07	0.71	80.3
37	41.85	68.27	0.44	77.5
40	38.78	55.90	0.38	84.6
43	38.03	61.87	0.47	78.0
46	35.08	62.60	0.55	77.6
49	38.39	58.24	0.51	81.5
52	36.67	62.28	0.50	76.6
55	35.20	55.84	0.56	78.5
58	35.77	60.47	0.59	82.3
61	35.07	44.08	0.67	77.3
64	36.32	56.32	0.63	77.4
67	38.40	55.23	0.62	78.2
70	36.86	49.11	0.66	82.9
73	36.48	54.50	0.61	79.4
76	35.95	50.42	0.69	78.8
79	36.79	51.45	0.56	82.1
82	36.48	57.55	0.57	81.4
85	37.38	52.54	0.66	74.6
88	36.84	60.76	0.49	75.3